Mem. Fac. Fish., Kagoshima Univ.
Vol. 22, No. 2, pp. 49～107 (1973)

Studies on the Production of Sea-Salt Particles on the Sea Surface*

Masaaki CHAEN**

Abstruct

Systematic observations of sea-salt particles in the lowest atmospheric layer over the oceans are carried out on board ships at sea. The salt-mass distributions of sea-salt particles, ranging from 10^{-11} gm to 10^{-7} gm are obtained by combined use of hand-operated impactors and rod samplers. The vertical distribution of sea-salt particles in the lowest several meters above the sea surface can be expressed by a modified form of Toba's equilibrium theory of sea-salt particles, by introducing the effective relative humidity. The feature of the mean salt-mass distribution of the number concentration of sea-salt particles, θ, at a height of 6 m for each wind force, for the salt-mass class of $\log m \leqq 2.25$ (m : the salt mass in 10^{-12} gm unit), is close to a straight-line segment on a logarithmic diagram, and it is expressed, as the first approximation, by Junge's form concerning the size distribution of aerosols in the atmosphere.

It is found that the number concentration of sea-salt particles, θ, increases linearly on a logarithmic diagram with a dimensionless variable, u_*L/ν, which represents the overall degree of the breaking of wind waves, where u_* is the friction velocity, L the significant wave length and ν the kinematic viscosity of air. The reference level of the production of sea-salt particles, z_1-surface, is newly introduced, and the number concentration of sea-salt particles at the z_1-surface, θ_1, is discussed. The character of the salt-mass distribution of θ_1 is always almost same, even though the wind speed and the state of sea surface may change, and the absolute value of θ_1 is proportional to u_*L/ν. The production rate of sea-salt particles, F_1, at the z_1-surface can be obtained from the value of θ_1 by $F_1 = w_s\theta_1$, where w_s represents the terminal velocity of sea-water droplet. The value of F_1 has the minimum at near $\log m = 3$. The character of the salt-mass distribution of F_1 is also always almost same as in the case of θ_1, and the absolute value changes with wind and sea states, in proportion to u_*L/ν.

In conclusion, the values of θ_1 and F_1 are presented for each class of salt mass as a function of u_*L/ν. Also, they are presented approximately as a function of wind speed alone, assuming the representative sea state as a function of wind speed.

Contents

---

* Dissertation for Doctor of Science (Tohoku University).

** Laboratory of Oceanography, Faculty of Fisheries, Kagoshima University, Kagoshima 890, Japan.

1. Introduction

The sea-salt particles originate from the sea surface, and take an important part in the condensation process of water vapor in the atmosphere. The sea surface maintains a perfectly definite surface, so far as the wind is weak. As the wind speed increases, wind waves develop, and the breaking of wind waves begins. Thus, the boundary surface between the air and the sea breaks and sea-water droplet, or, sea-salt particles* are produced. The breaking of wind waves is related to the process of the transfer of momentum from wind to wind waves, to the turbulence in the sea water, and to the drift current. Besides, the breaking of wind waves affects the rate of evaporation from the sea surface, and in turn the heat exchange between the air and the sea, since air bubbles and sea-salt particles are produced on the sea surface. In this manner, the breaking of wind waves is related to many problems of the air-sea boundary processes, and the corresponding production of sea-salt particles has a similar significance. Moreover, there is a plan aiming to estimate the distribution of wind over global oceans from a satellite observation of radar return from the sea surface (Moore and Pierson, 1971) and a problem of anthropogenic chemical films on the sea surface has become of major interest, with the development of human activity (Duce et al. 1972). The wave breaking apparently plays a part in these problems also.

It is necessary, therefore, to clarify the mutual relations among such quantities as the sea-salt particles, the overall degree of the breaking of wind waves and the prevailing wind over the sea surface.

The mechanism of production of sea-salt particles is investigated by Woodcock et al. (1949, 1953), Kientzler et al. (1954), Knelmen et al. (1954), Mason (1955), Blanchard and Woodcock (1957) and Blanchard (1963) by means of laboratory experiments or observations at the sea. Hayami and Toba (1958) and Toba (1959, 1961) carried out a series of experiments of the production of water droplets in a wind-wave tunnel, together with theoretical considerations, and clarified the mechanisms of air bubble entrainment and of the production of water droplets. There is few observation on the actual sea surface concerning these problems. The observations

* In this article, the term "sea-salt particles" is used in the meaning including all the states of droplets of sea water, droplets of condensed sea-salt solution, and dry sea-salt particles.

of sea-salt particles near the sea surface were carried out by Fournier d' Albe (1951) in Monaco Bay, by Moore (1952) and Moore and Mason (1954) in the Atlantic Ocean. Recently, Kikuchi and Yaura (1970) observed sea-salt particles on board ice breaker "Fuji" from Tokyo to Antarctica. Unfortunately, all of these observations were carried out at only one height above the sea surface.

Toba (1965, 1965a, 1966) proposed a theory of the vertical distribution of sea-salt particles, and estimated the amount and production rate of sea-salt particles at the sea surface, by synthesizing the data of sea-salt particle observation at cloud levels by Woodcock (1953) and other investigations. In order to compare the theory with the actual data, Toba et al. (1971) carried out an observation of the vertical distribution of sea-salt particles at the Shirahama Oceanographic Tower Station in Tanabe Bay, together with observations including wind profiles and wind waves. Further, Toba and Chaen (1969), and Toba, Okuda and Chaen (1971) carried out systematic observations including the wind, wind waves, the breaking of wind wave and sea-salt particles, on board the R. V. Hakuhō Maru. Some of the analysis, especially concerning the breaking of wind waves, have been published by Toba and Chaen (1973).

In the present article, a further analysis is presented to determine the amount and the vertical distribution of sea-salt particles in the lowest atmospheric layer above the sea surface, and their production rates on the sea surface, by synthesizing the above mentioned data from the Hakuhō Maru, the data obtained by the present author on board the Kagoshima Maru (Chaen, 1971, 1972), and the data from the Shirahama Oceanographic Tower Station by Toba et al. (1971).

2. Observations

2.1. Procedure of observation of sea-salt particles

2.1.1. Sampling surface of sea-salt particles

In the observation of sea-salt particles, it is necessary to obtain the salt mass contained in a particle and the number of sea-salt particles in each class of salt mass. There are some methods used for the purpose, for instance, the method of micro chemical analysis, the isopiestic method and the optical method. The method of micro chemical analysis is extensively used in the case where the large number of observations of sea-salt particles in the class of salt mass larger than 10^{-11} gm. In the present study, this method was used.

The sampling surface is a gelatin layer on the film containing silver dichromate gel, and when a sea-salt particle is collected on the film surface, it diffuses into the gelatin layer, and the chlorine ion precipitates as silver chloride, producing a white circular spot on the reddish brown base of the film. The mass of chlorine can be determined by measuring the size of the white spot.

In practical, it is convenient to use the method of Toba and Tanaka (1967), which is an improved method of Farlow's (1954, 1957, 1958). The preparation procedures of this sampling surface are as follows. As the basic film for the halide-ion sensitive film, a commercial Fuji Gravure Safety Film Normal (cabinet size), having a gelatin layer of 11.0 μ in thickness, is used. The film is put into a fixative for about 20 minutes for removing sensitizer, and it is fully washed with distilled water. The film becomes a colorless transparent film with gelatin layers on both sides. The film after washing is dried in a glass desiccator with silicagels for about one day. Two kinds

of reagent solution are prepared : one is a mixed solution of 0.5% sodium dichromate and 2% polyvinyl alcohol in distilled water, the other is a solution of 5% silver nitrate. The film after being dried is dipped into the first solution for 2 minutes, drained for 15 sec, dipped into the second solution for 2 minutes, drained for 15 sec, and coarse sediments on the surface are rubbed off with a soft sponge in a distilled water for 30 sec, and it is dried in a glass desiccator covered with a black hood, for the film is slightly photosensitive. This is the gelatin film containing reddish brown sediment of silver dichromate, and may be used by cutting it to a convenient size.

After sampling the sea-salt particles on the reagent film, the film is put on a filter paper in the glass desiccator which keeps the inside slightly below 100% in the relative humidity, and the white halos of silver chloride on the film is fully developed. After developing, the film is dried in the glass desiccator with silicagels, covered with a black hood. Then, it is essential to cover the film with a transparent coating by dipping the dried film into a solution of about 2% collodion, in order to prevent further contamination by salt particles.

In order to determine the salt mass of a white halo, a microphotograph with 60 times magnification is taken, and finally, a 100 times enlarged print of the photograph is made relative to the original white halo on the reagent film. The salt mass is easily determined by the transparent scale which calibrate the relation between the dry masses of sea-salt particles and the sizes of white halos, as described in Toba and Tanaka (1967), and the particle number was obtained for each class of the range of $\log m = 0.25$ (the salt mass contained, m, is in 10^{-12} gm unit).

As to the method of measuring the diameter in situ of sea-salt particles when sampling, the sampling surface of MgO on a slide has been used (May, 1950). The magnesium oxide layer is obtained by moving burning magnesium ribbon to and fro under a metal slide or a glass slide. The slide surface becomes snow white by the soot of magnesium. Through a microscope, the situation of sea-salt particles on the MgO surface shows a striking analogy to those made by stones falling into snow. The ratio of diameter of water droplet to the hole produced on the magnesium oxide layer is about 0.86. The size of water droplet can be determined from the diameter of the hole measured by moving microscope with 1 μ vernier.

2.1.2. Procedure of sampling of sea-salt particles

A hand-operated jet impactor described by Toba and Tanaka (1967) was used. The design is shown in Fig. 1. The impactor has an air intake with an orifice of 1 mm diameter (Mark A). By use of a 100 cc medical syringe (Mark G), an air jet is formed at the orifice, and sea-salt particles impact on a circular area of 1 mm diameter on the reagent film (Mark D). By rotating stage C by use of a handle (Mark F), six different volumes of air may be sampled successively as shown in the left hand part of Fig. 1. When using the impactor, the air intake of the impactor is directed against the wind, and the syringe is drawn at a speed of 3 sec per 100 cc or a little faster. In this case, a jet speed through the air intake is about 42 m sec^{-1} or faster. According to the theoretical and experimental studies by Ranz and Wong (1952), it is concluded that sea-salt particles larger than 1 μ diameter are collected perfectly by the jet impactor with a round orifice of 1 mm diameter when the jet speed is higher than 40 m sec^{-1}.

However, larger sea-salt particles in a low concentration have little chance to be caught by the impactor, since the impactor collects particles contained in a certain volume of air. So, the

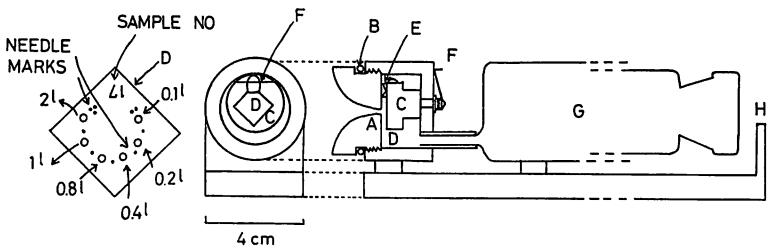

A : AIR INTAKE
B : O RING
C : FILM STAGE
D : REAGENT FILM
E : FILM HOLDER
F : HANDLE
G : 100 CC SYRINGE
H : STOPPER

Fig. 1. Design of the hand-operated impactor for measurement of sea-salt particles (Toba and Tanaka, 1967).

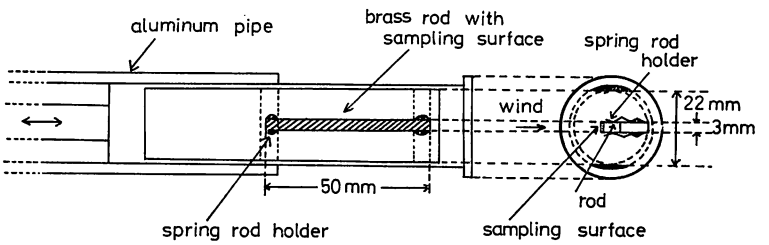

Fig. 2. Head part of the rod sampler for the measurement of sea-salt particles, showing a 3-mm wide film mounted in the window (Toba et al., 1971).

other sampler which selectively collects the larger sea salt-particles was simultaneously used. The sampler was made of a aluminium pipe of 3 cm in diameter and 3 m long. The top of the pipe has a structure shown in Fig. 2, and a 3-mm or 5-mm wide reagent film or the MgO surface is hold in the window. When the window is open, the sampling surface is exposed at right angles to the wind for a measured time, and sea-salt particles impact on it. This sampler is named the rod sampler, and was first used during the Hakuhō Maru Cruise KH-69-3 (Toba and Chaen, 1969). The efficiency of impaction of the film ribbon had been studied theoretically or empirically by Ranz and Wong (1952), Langmuir and Blodgett (1948). In the present observation, however, as will be described in section 2. 3, the efficiency obtained by the observation was not always in agreement with the theoretical results by them, it was found that the efficiency of impaction was about 80% or more for the sea-salt particles larger than 1.8×10^{-10} gm ($\log m = 2.25$). The detailed procedures of the observations on board ships at sea will be described in the next section.

2. 2. Observations of sea-salt particles on board ships at sea

2. 2. 1. Observations on board the Kagoshima Maru

The observations of sea-salt particles on board the Kagoshima Maru, Kagoshima University were carried out at the observation stations of the two international oceanographic programs. One was the International Indian Ocean Expedition (IIOE) in December, 1963 through January,

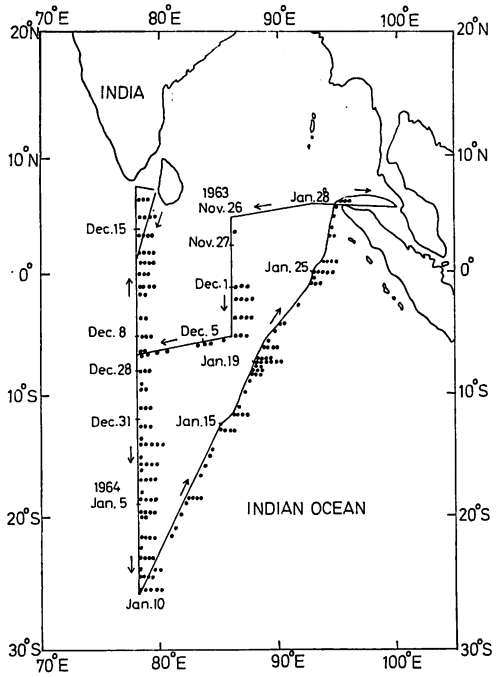

Fig. 3. Map showing the observation stations of the Kagoshima Maru in the IIOE Cruise. Black circles indicate the location and the number of observations of sea-salt particles.

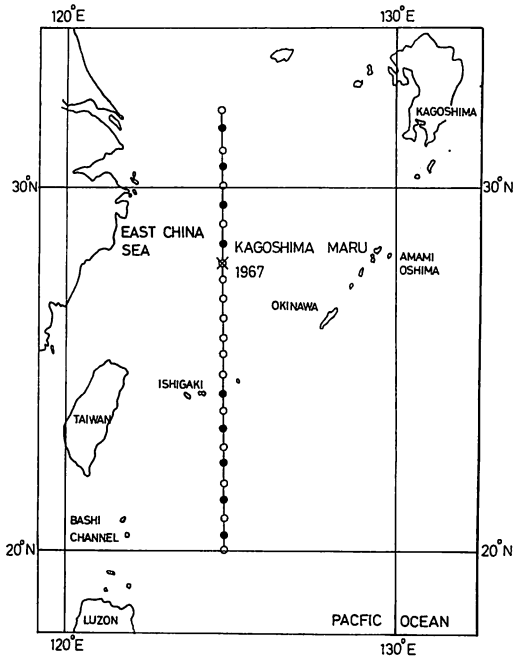

Fig. 4. Map showing the observation stations of the Kagoshima Maru in the CSK Cruise. Circles indicate the stations of oceanographic observations and sea-salt particles observations. Cross indicates the anchored station for the hourly observations of sea-salt particles for two days.

1964 and the other was the Cooperative Study of the Kuroshio (CSK) in August, 1967.

In the Indian Ocean, as shown in Fig. 3, on two or three occasions observations were carried out at each station of oceanographic observation on board while the ship was drifting, and the number of observations totaled about 300. In the East China Sea, the hourly observations of sea-salt particles for two days were carried out at the anchored station (cross mark station), as shown in Fig. 4, besides those at each station of the oceanographic observation. All of these observations were carried out for the vertical distribution of sea-salt particles, and the impactor was used.

The sampling places on board the ship were at three heights, as shown in Fig. 5, namely, the flying bridge deck of about 9 m in height above the sea surface, the boat deck of about 4 m and on the bulwark of the main deck of about 2 m, and for the hourly observation in the East China Sea, the height of about 1 m above the sea surface was added.

The time required for the observation of sea-salt particles at one height was about one minute, and then, the total time took less than several minutes for one vertical observation of the three or four heights including the time required for moving from one sampling place to another. As the sampled air volume, two or three of the volume of air was adopted among various volumes, such as 50 cc, 100 cc, 200 cc, 400 cc, 800 cc and 1, 000 cc, according to the states

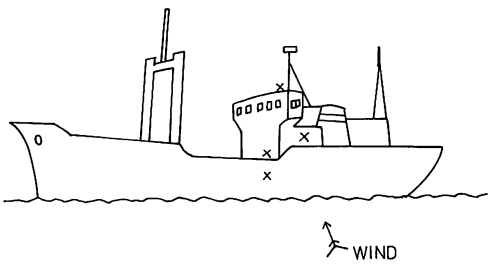

Fig. 5. Sampling places (cross marks) on board the Kagoshima Maru.

of sea surface.

The surface meteorological data at the time of sampling: the wind, the dry and the wet-bulb temperatures and the sea-surface temperature were measured. The photographs of the condition of sea surface were also taken. The wind speed was read from the indicator of a cup anemometer equipped at the 14-m level on the ship. The wind speed at the 10-m level was estimated from the 14-m level value by the use of the logarithmic law, with the friction coefficient, C_D, of 1.6×10^{-3}. The relative humidity was calculated from values of the dry and the wet-bulb temperatures measured by use of an Assmann ventilated psychrometer at the 9-m level on the ship. The values of the number concentration of sea-salt particles, the wind speed at the 10-m level, and the relative humidity at 9-m level observed in the Indian Ocean were shown in figures by Chaen (1971). The observations on board the Kagoshima Maru were taken under conditions of relatively light wind specd, i.e., from calm to 12 m sec^{-1} in the Indian Ocean, and from 2.0 m sec^{-1} to 5.5 m sec^{-1} for the the hourly observations in the East China sea.

2.2.2. Observations on board the Hakuhō Maru

In July of 1969 and 1970, as a part of the GARP (Grobal Atmospheric Research Program), the observations of the air-sea boundary processes including sea-salt particles, the wind, wind waves and breaking of wind waves were carried out on board the Hakuhō Maru of Ocean Research Institute, University of Tokyo, in the East China Sea and other districts. The two cruises

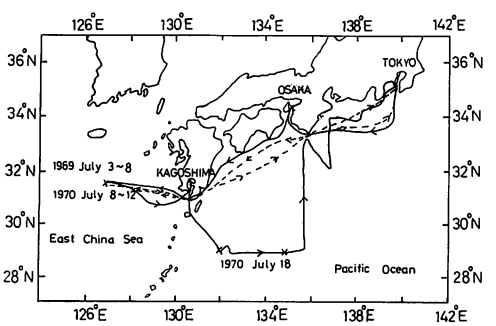

Fig. 6. Map showing the observation stations of sea-salt particles (cross marks) and tracks of the Hakuhō Maru in the GARP Cruise (dashed line) and the 2nd GARP Cruise (solid line).

in 1969 and 1970 were called the KH-69-3 Cruise (GARP Cruise) and the KH-70-3 Cruise (2nd GARP Cruise), respectively. The observation stations and her tracks in the two cruises are shown in Fig. 6. The preliminary reports of the observations were already published in the cruise reports of Ocean Research Institute, University of Tokyo, by Toba and Chaen (1969) and Toba, Okuda and Chaen (1971), and concerning the breaking of wind wave field by Toba and Chaen (1973).

In the KH-70-3 cruise on her sea way to the East China Sea, Typhoon 7008 (Oruga) hit Japan on July 5, 1970 and the ship was anchored off Fuke, Osaka Bay for 24 hours, and the observation was carried out until the wind speed reached 16.6m sec^{-1} at 10-m level, without rain. On the other hand, there were cases where the sea surface was like a mirror under the calm conditions, so we experienced a wide range of the sea conditions in these cruises.

The observations of vertical distribution of sea-salt particles were taken at three heights, namely, the compass bridge deck of about 13 m in height above the sea surface, the hole near the starboard bow on the bridge deck of about 6 m or 5 m, and the starboard on the main deck of about 3 m or 2.5 m (Fig. 7). In the observation on board the Hakuhō Maru, both the impactor and the rod sampler were used in some cases simultaneously, and in some cases separately. The rod sampler with the 5-mm wide film was used in 1969, and rod samplers with mainly 3-mm

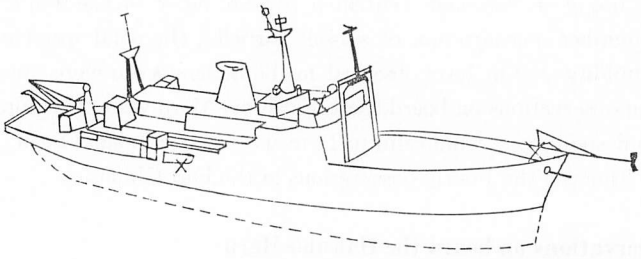

Fig. 7. Sampling places (cross marks) on board the Hakuhō Maru.

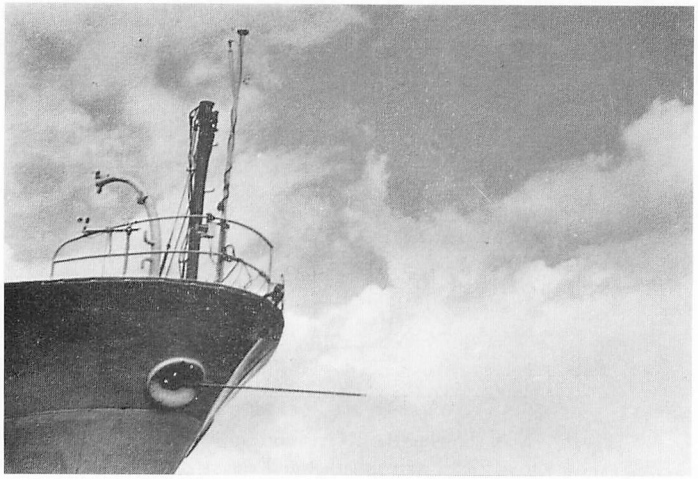

Fig. 8. A view of the sampling of sea-salt particles by the rod sampler at a height of 6 m above the sea surface on board the Hakuhō Maru.

one were used in 1970. A view of the conditions of the observation by the use of the rod sampler at a height of 6 m is shown in Fig. 8. The sampler is projected as far as possible from the body of the ship, and its window is opened to expose the film to the air at right angles to the flow for a measured time. The exposed time interval was empirically decided, for instance, 300 sec for a wind speed of 3.3 m sec^{-1}, 180 sec for 6.0 m sec^{-1} and 5 sec for 16.6 m sec^{-1}, in order to get a significant number of sea-salt particles and also to avoid the masking of particles.

The observations for the check of the impaction of efficiency, and the measurement of the diameter in situ of sea-water droplet by the MgO surface were carried out at the height of 6 m above the sea surface. In the observation by use of the impactor, six spots of sea-salt particles were taken on the reagent film at one height, for different air volumes or for the same ones, in order to obtain the retention factor for the impactor and to get the counted particle number of over several tens (Toba and Tanaka, 1968). In order to obtain the efficiency of impaction of the rod sampler, the simultaneous observation by the impactor and the rod sampler was made. These results will be stated in the next section.

Surface meteorological data, such as the wind, the air temperature, the dew point and the sea-surface temperature were obtained from the records of ship's equipments. The wind speed at the 10-m level was estimated from the 20-m level value by the logarithmic law. The relative humidity was calculated from the air temperature and the dew point. As to wind waves, the period of significant waves was measured by the use of a stop watch, by watching some marks on the water surface, such as bubbles produced by the breaking of wind waves. Furthermore, the breaking of wind waves was evaluted as the percentage of the white breaking area to the area of sea surface, by use of the color slide pictures, including the horizon near the top of the picture taken at a fixed height of 14 m, in the four directions relative to the direction of wind

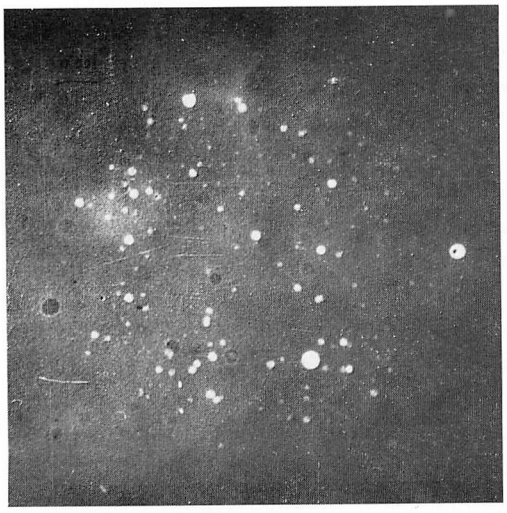

Fig. 9 (a)

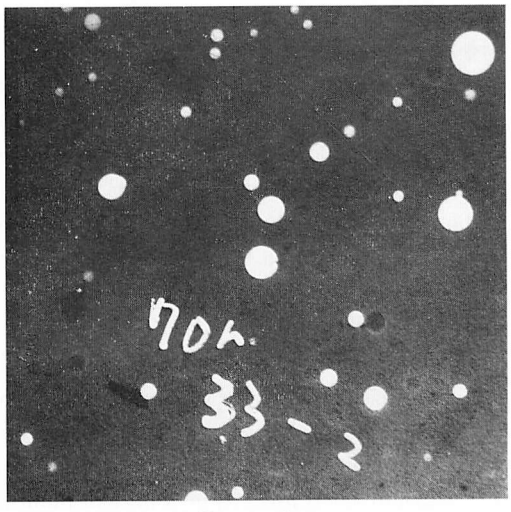

Fig. 9 (b)

Fig. 9. Examples of the sampling surface of the reagent film with white circular spots developed by sea-salt particles by (a) the impactor and (b) the rod sampler. The largest spot on the film by the impactor and the rod sampler has 40.4 μ and 100 μ in diameter (3.7×10^{-10}gm and 2×10^{-9}gm salt mass contained), respectively.

Fig. 10. Example of the sampling surface of the MgO film with the craters developed by sea-salt particles. The scale indicates 100μ.

waves. The pictures were already analyzed, and Toba and Chaen (1973) showed the interrelationships among the variable governing the overall degree of the breaking of wind waves, the percentage of the breaking area, and the number concentration of sea-salt particles.

The reagent films after sampling were carefully treated according to the procedure described in section 2. 1. 1. In Fig. 9 are shown the white circular spots of sea-salt particles on the reagent film obtained by the use of the impactor, and of the rod sampler, and in Fig. 10 is shown the craters of sea-salt particles produced on the MgO surface. The white circular spots collected by the impactor were measured and counted for all six spots and those by the rod sampler were treated as about 10 to 30 sheets of 100 times enlarged microscopic photographs for each observation. The original area of one sheet of the microscopic photograph by the rod sampler is 1×10^{-2} cm^2. When the microscopic photographs of the film of the rod sampler were taken, the visual field of microscope was succesively moved on the film, in order to obtain a series of prints including 10 to 30 sheets. This was to avoid the personal selection for the situation of the distribution of white circular spots. By the above mentioned procedure, the counted particle number at one observation became large and very reliable data of sea-salt particles were obtained.

The number concentration of sea-salt particles, θ, for the ranges of log $m = 0.5$ obtained during the KH-69-3 and KH-70-3 cruises are shown in Table 1. The wind speed, the relative humidity, the period of significant wave and the class of wind waves at the time of observation of sea-salt particles are shown in Table 2. Several examples of the salt-mass distribution of θ for the ranges of log $m = 0.25$ are shown in Fig. 11. The number concentration of sea-salt particles, obtained by the impactor is high in the class of salt mass of log $m \leqq 2$, and that of the rod sampler is low. The values of number concentrations by the two samplers fairly agree in the class of salt mass of log $m = 2\sim 2.5$, as shown in the figures. A wide range of the salt-mass distribution of sea-salt particles from log $m = 1$ (about 8 μ in diameter, as a sea-water droplet) to log $m = 5$ (about 175 μ in diameter) have been able to be obtained, using the two kinds of samplers at the same time.

Table 1. Observational data of sea-salt particles.

Run no.	Height (m)	Sampler	Number concentration of sea-salt particles, θ ($\times 10^{-3}$ cm^{-3})							
			$\log m =$ 1	2	3	4	5			
1 (July 1, 1969)	13	Imp.	94.3	55.0	2.64	1.75				
	5	Imp.	309	49.7	6.18					
2	13	Imp.	880	288	33.5	2.35				
	10	Rod		8.67	16.7	6.45	1.41		0.202	
	5	Imp.	257	185	31.2	1.50				
	5	Rod	0.282	16.1	23.9	10.4	1.98			
3	13	Imp.	192	133	47.3					
	13	Rod		5.43	12.6	6.99	2.53	0.388		
	7.4	Rod		6.74	17.7	10.6	2.84	0.355		
	5	Imp.	170	101	37.0	7.40				
	5	Rod	0.414	15.7	18.0	11.6	1.86	1.24		
4 (July 2)	13	Imp.	66.2	68.5	23.6	3.04				
	5	Imp.	69.5	72.1	21.2	2.64				
5 (July 3)	13	Imp.	43.8	13.0	3.26					
	5	Imp.	26.4	8.27						
6	13	Imp.	311	125	22.2	1.00				
	13	Rod	3.30	13.4	4.61	0.713	0.250			
	6	Imp.	204	123	25.3					
	6	Rod	0.235	12.4	5.79	0.626				
7 (July 5)	13	Imp.	261	124	9.36					
	13	Rod	3.24	26.8	12.6	1.26				
	6	Imp.	697	237	23.1	6.16				
	6	Rod	1.91	16.6	10.4	2.97	1.08		0.106	
8 (July 6)	13	Imp.	150	20.6	2.65					
	13	Rod	8.95	24.5	13.9	6.27	0.783			
	6	Imp.	484	93.6	10.6					
	6	Rod	0.693	9.39	9.50	3.24	0.770	0.077		
9 (July 7)	13	Imp.	245	28.1	2.34					
	13	Rod	4.48	8.62	0.793					
	6	Imp.	332	56.2	11.7					
	6	Rod	13.1	26.9	3.80	0.295				
	2.5	Imp.	653	337	50.6	3.30				
	2.5	Rod	3.58	25.0	10.9	0.325				
10	13	Imp.	583	333	20.0					
	13	Rod	8.60	32.4	15.9	1.50				
	6	Imp.	636	309	49.7					
	6	Rod	11.8	30.1	11.6	0.656				
	2.5	Imp.	526	277	39.7	3.30				
	2.5	Rod	0.699	14.3	11.9	1.96	0.210	0.070	0.210	
10′	0.3	Rod	2.93	50.6	35.6	7.54	0.418		0.418	
	0.3	Rod	1.36	20.4	20.3	4.51	0.788	0.113	0.113	
11	13	Imp.	297	85.6	1.84	0.493	0.493			

Table 1. (Continued)

Run no.	Height (m)	Sampler	Number concentration of sea-salt particles, θ ($\times 10^{-3}$ cm^{-3})								
			$\log m =$ 1	2	3	4	5				
11 (July 7, 1969)	13	Rod	29.0	30.1	17.3	5.61	1.05		0.051		
	6	Imp.	424	89.0	25.3	1.34					
	6	Rod	19.2	49.2	26.8	9.62	1.16	0.155			
12 (July 8)	13	Imp.	216	37.2	3.04	0.520		0.493			
	13	Rod	33.7	39.3	24.8	13.3	3.20	0.388			
	6	Imp.	855	274	27.6	6.77					
	6	Rod	2.04	18.4	20.6	14.4	4.55	0.467	0.311		
	2.5	Imp.	696	313	86.0	29.8					
	2.5	Rod	2.95	30.3	29.4	16.3	7.57	1.66			
13	13	Imp.	421	93.9	36.8	12.4					
	13	Rod	3.58	29.7	24.6	16.2	8.42	2.10	0.421		
	6	Imp.	213	143	34.6	6.52	3.74				
	6	Rod		12.5	24.0	16.2	9.34	2.51	0.228		
	2.5	Imp.	614	215	114	35.0	19.5	1.25			
	2.5	Rod	1.51	37.6	50.8	33.5	21.5	1.88	0.752		
14 (July 9)	13	Imp.	150	50.8	18.5	0.293					
	13	Rod	0.654	9.01	7.66	2.70	0.872	0.218			
	6	Imp.	220	81.5	31.1	3.99					
	6	Rod	0.863	7.09	7.03	2.40	0.432	0.192			
15 (July 10)	13	Imp.	96.6	32.9	11.0	0.50					
	6	Imp.	84.4	80.2	19.2	2.89		0.293			
	6	Rod	0.038	3.01	8.71	4.09	1.08	0.076			
2	6	Rod	0.322	9.74	12.8	5.39	2.17	0.162	0.081		
3 (July 5, 1970)	6	Imp.	147	86.8	14.8	2.63	0.240				
	6	Rod	0.296	12.7	16.3	11.2	5.23	1.29	0.198		
4	6	Imp.	357	160	47.9	11.5	5.21	2.27			
	6	Rod	0.253	13.1	29.3	17.6	10.4	3.53	0.758	0.084	
5	6	Imp.	307	149	55.3	11.1	3.10				
	6	Rod	9.25	23.4	21.9	13.9	7.85	2.29	0.545		
6	6	Imp.	330	106	17.5	7.05	2.20				
	6	Rod	8.76	25.9	30.9	16.7	10.2	3.55	0.591		
7	6	Imp.	410	109	17.7	2.60					
	6	Rod	0.750	20.1	32.3	22.9	11.3	3.63	0.500		
8	6	Imp.	348	112	20.2	2.57					
	6	Rod	17.3	70.8	61.3	33.3	22.3	7.24	1.26		
9	6	Imp.	399	133	21.0	1.90	1.36				
	6	Rod	7.60	47.7	61.6	43.5	23.9	8.12	1.31	0.262	
10	6	Rod	20.4	65.3	79.5	52.9	32.2	18.2	5.49	0.818	0.168
11	6	Rod	17.2	55.6	62.5	52.6	36.2	18.7	9.02	1.61	0.261
12	6	Rod	19.4	94.9	114	88.7	31.5	16.9	7.32	1.78	0.245
13 (July 6)	6	Imp.	82.5	17.2	1.14	0.560					
	6	Rod	2.02	8.17	6.71	3.23	0.728	0.081			

Table 1. (Continued)

Run no.	Height (m)	Sampler	Number concentration of sea-salt particles, θ ($\times 10^{-3}$ cm^{-3})								
			$\log m =$ 1	2		3		4		5	
14	6	Imp.	49.9	16.2	1.29						
(July 6, 1970)	6	Rod	2.04	7.50	6.10	2.13	0.367				
15	6	Imp.	54.5	26.5	7.52	1.05	0.103				
	6	Rod	0.130	1.44	1.83	1.30	0.235	0.047			
16	6	Imp.	77.8	33.0	11.1						
	6	Rod	0.092	5.04	6.46	1.76	0.248	0.052			
17	13	Rod		0.235	1.38	0.511	0.236	0.020			
(July 8)	6	Rod		0.386	1.93	0.861	0.181	0.023			
	3	Rod		0.371	2.15	0.775	0.168				
19	13	Imp.	67.6	16.6	5.19	0.303					
	6	Imp.	58.0	16.7	4.33	0.185					
	3	Imp.	60.9	15.6	4.86	0.455	0.115				
20	13	Imp.	53.3	17.3	4.24	0.103	0.307				
	6	Imp.	47.5	20.7	2.99	0.460					
	3	Imp.	50.3	11.2	5.04	0.793	0.103				
21	13	Imp.	63.0	16.9	3.81	0.173					
	6	Imp.	53.0	19.8	4.10	0.103	0.103				
	3	Imp.	107	60.2	37.1	7.42	1.86				
21′	3	Imp.	53.6	14.3	4.52	0.560					
22	13	Imp.	52.6	22.3	5.25	0.703	0.173				
(July 9)	6	Imp.	42.8	17.1	10.4	1.41					
	3	Imp.	26.6	12.8	5.46	0.498					
23	0.7	Imp.	33.1	17.4	5.95	0.797	0.267				
24	13	Imp.	30.8	15.3	4.92						
	6	Imp.	32.7	12.4	3.66	0.103					
	0.7	Imp.	44.7	18.1	4.16	4.02	1.14				
25	13	Imp.	15.6	6.14	2.20	0.277					
	6	Imp.	19.4	7.08	2.03	0.173	0.160				
	3	Imp.	97.0	65.2	60.9	15.9	2.11	0.525			
26	13	Rod	0.355	4.67	5.09	1.74	0.293	0.031			
(July 10)	6	Rod		0.097	0.484	0.276	0.970				
	3	Rod	0.420	6.26	9.89	4.12	0.798	0.336	0.063		0.021
27	13	Rod	0.932	8.38	7.72	2.13	0.329	0.055			
	6	Rod	3.66	13.8	10.1	2.91	0.285				
	3	Rod	0.387	9.76	12.7	4.89	1.30	0.414	0.083		
29	6	Imp.	347	61.2	4.64						
(July 11)	6	Rod	0.140	11.3	18.5	5.12	0.841	0.105			
	6	Rod		1.15	9.11	3.49	0.485	0.030	0.030		
30	13	Rod	0.145	2.23	9.76	3.04	0.492				
	6	Rod		0.707	7.10	3.30	0.236	0.034			
	3	Rod	0.073	3.56	10.3	3.49	0.472	0.073			
31	13	Rod	3.43	2.54	18.8	7.28	2.57	0.515	0.086		

Table 1. (Continued)

Run no.	Height (m)	Sampler	Number concentration of sea-salt particles, θ ($\times 10^{-3}$ cm^{-3})								
			$\log m =$ 1	2	3	4	5				
31 (July 11, 1970)	6	Rod	1.11	15.4	17.7	7.37	2.63	0.407	0.037		
	3	Rod	0.325	7.84	16.1	8.11	3.36	0.812	0.378	0.054	
32	13	Rod	0.896	10.7	11.9	5.99	1.39	0.285	0.162		
	6	Rod	0.032	2.52	7.63	4.66	1.63	0.224	0.096		
	3	Rod	0.514	3.15	5.93	3.70	0.93	0.412			
33	13	Imp.	213	84.8	30.6	9.73	2.78	1.39			
	6	Imp.	225	128	45.9	11.1					
	3	Imp.	234	165	84.8	16.7	4.17				
34	13	Imp.	303	106	32.3	4.98	0.306				
	6	Imp.	297	115	43.8	4.09					
	3	Imp.	368	202	123	29.1	3.62				
37 (July 12)	6	Imp.	363	94.8	5.48						
	6	Rod	42.7	46.4	23.4	5.29	0.603	0.079			
	6	Rod	6.30	36.1	20.5	6.26	1.56	0.173			
38 (July 16)	6	Imp.	123	28.6	6.46	0.695					
	6	Rod		0.101	1.66	0.404	0.101				
39	6	Imp.	55.8	32.3	10.0	0.230					
40 (July 17)	6	Imp.	139	44.6	9.92	1.52	0.200				
	6	Rod		0.029	0.724	0.388	0.058				
41	6	Imp.	164	64.5	36.5	3.50	0.850				
	6	Rod		0.584	3.08	1.76	0.372	0.080	0.027		
42	6	Imp.	121	61.6	19.5	1.07					
	6	Rod		0.478	3.15	1.41	0.173	0.058			
43	6	Imp.	160	59.3	27.5	3.01					
	6	Rod		0.956	6.96	2.24	0.545	0.059			
44	6	Rod		0.882	3.80	1.42	0.441		0.018		
45	6	Imp.	164	65.3	9.36	1.38					
	6	Rod		0.053	0.476	1.32	0.159				
46 (July 18)	6	Imp.	137	59.8	25.0	2.75					
	6	Rod		0.434	2.62	1.30	0.452	0.017			
47	6	Imp.	137	61.9	17.1	0.880	0.230				
	6	Rod	0.017	1.94	6.02	2.15	0.580	0.083			
48	6	Imp.	250	90.6	33.8	3.94	1.94				
	6	Rod		1.22	7.39	3.75	1.08	0.180			
49 (July 19)	6	Imp.	671	190	36.5	12.8					
	6	Rod	1.71	20.4	37.2	16.3	5.59	1.08	0.271		
50	6	Rod		0.866	13.6	9.81	3.24	0.866	0.144		
51	6	Rod		3.75	19.5	10.6	4.18	0.649	0.144	0.072	0.144
52	6	Imp.	687	232	61.1	5.56	1.39	2.78			
	6	Rod	1.10	24.2	49.5	15.3	1.11	0.892	0.206		
	6	Rod	0.147	4.33	25.7	10.3	3.97	0.882	0.147		
53	6	Imp.	976	290	93.7	14.8					

Table 1. (Continued)

Run no.	Height (m)	Sampler	Number concentration of sea-salt particles, θ ($\times 10^{-3}$ cm^{-3})								
			$\log m =$ 1	2	3	4	5				
	6	Rod	510	59.6	62.5	19.8	3.90	0.751	0.150		
56	6	Imp.	1080	298	66.6	11.1	1.39				
(July 19, 1970)	6	Rod	1.71	36.9	43.5	15.6	4.28	0.997			
58	6	Imp.	368	112	29.4	3.03	0.306				
(July 20)	6	Rod	6.08	19.0	12.7	2.90	0.246				
60	6	Imp.	28.6	16.9	2.59	0.306					
	6	Rod	1.26	2.26	1.06	0.151	0.013				0.013
61	6	Imp.	2.78	2.50	0.306						
	6	Rod	0.244	0.654	0.483	0.060	0.021	0.007			

Table 2. Surface meteorological and wind wave data at the time of observation of sea-salt particles. The U_{10} represents the wind speed at 10-m level, RH the relative humidity, T the significant wave period. Data of scale of wind waves is reprinted from ship's log of the Hakuhō Maru.

Run no.	Date	Time*	U_{10} (m sec^{-1})	RH (%)	T (sec)	Wind waves (scale)
1	July 1, 1969	09 : 30	9.1			5
2		14 : 05～14 : 25	9.8			4
3		17 : 10～17 : 50	8.3～10.5			4
4	July 2	08 : 20～09 : 00	4.3～4.7			2
5	July 3	08 : 25～08 : 45	4.9	95		2
6		15 : 02～15 : 25	7.4～8.8	94		3
7	July 5	17 : 10	7.2～8.8	95～97		3
8	July 6	13 : 40～13 : 53	8.7～9.0	98		3
9	July 7	14 : 25～14 : 52	4.7～5.6	95		1～2
10		15 : 20～15 : 45	6.1～6.5	93		2～3
10′		15 : 55～16 : 04	6.1～6.5	93		3
11		20 : 11～20 : 25	10.0	95		4
12	July 8	09 : 04～09 : 15	12.1～12.6	92～97		5
13		10 : 49～11 : 11	12.8	81		5
14	July 9	19 : 27～19 : 47	7.1～8.2	81		2～3
15	July 10	08 : 56～09 : 20	1.2～3.5	70		0

* Time of observation for sea-salt particles.

Table 2. (Continued)

Run no.	Date	Time*	U_{10} (m sec^{-1})	RH (%)	T (sec)	Wind waves (scale)
2	July 5, 1970	08 : 54	7.3	74		
3		10 : 20～10 : 22	7.9	77	3.72	
4		12 : 17	9.3	76	3.90	
5		12 : 55	10.7	71	4.40	
6		14 : 10	13.9	76	4.50	
7		14 : 27	13.0	80	4.50	
8		15 : 25～15 : 27	11.2	76	4.97	
9		15 : 44	11.2	74	4.98	
10		17 : 07～17 : 08	13.0	79	5.50	
11		17 : 59～18 : 00	14.4	76	6.25	
12		18 : 56～18 : 57	16.6	85	6.07	
13	July 6	10 : 52	3.8	72	(1.5)**	4
14		13 : 17～13 : 18	3.8	73	2.17	3
15		15 : 14	3.2	64	(0.44)	2
16		17 : 44～17 : 45	3.3	83	1.78	1
17	July 8	10 : 15	5.1	87	1.41	3
18		12 : 35	4.9		1.62	
19		14 : 45	4.4	76	1.32	2
20		16 : 13～16 : 35	4.2	81	1.11	2
21		18 : 18	3.7	80	1.30	2
21′		19 : 00	3.7	80		2
22	July 9	08 : 38	3.3	90	1.32	2
23		10 : 00	3.5	93		2
24		11 : 03	2.8	90	1.13	2
25		18 : 23	1.9	91	(0.6)	2
26	July 10	09 : 11	7.0	99	1.26	2
27		10 : 56	7.6	96	1.87	2
29	July 11	08 : 10～08 : 11	6.4	97	3.05	4
30		08 : 40	5.8	94	3.03	3
31		09 : 39	7.9	99	3.63	3
32		11 : 14	6.1	88	3.08	3
33		16 : 08	2.4	92	(4.96)**	3
34		16 : 45	0.8	92		3
37	July 12	16 : 00	8.0	96	2.54	3
38	July 16	08 : 27	4.7	93	1.90	2
39		13 : 00	2.3	82		2
40	July 17	08 : 15～08 : 16	4.4	86	1.63	3
41		11 : 05	6.1	87	2.28	2
42		13 : 18	6.2	82	2.69	3
43		15 : 08	6.1	80	2.57	3

** T-values for swells.

Table 2. (Continued)

Run no.	Date	Time*	U_{10} (m sec^{-1})	RH (%)	T (sec)	Wind waves (scale)
44	July 17, 1970	17 : 30	3.7	83		4
45		17 : 49	4.0	83	1.91	4
46	July 18	10 : 07	6.2	83	2.56	3
47		12 : 25	6.7	82	2.65	3
48		15 : 19	6.9	76	2.82	3
49	July 19	08 : 24	9.7	93	3.88	5
50		09 : 04	10.4	90		5
51		09 : 20	10.4	90		
52		09 : 32～09 : 33	9.8	93	3.55	5
53		12 : 40	8.8	95	3.64	5
56	July 19	17 : 08	8.7	97	2.64	4
58	July 20	08 : 49	6.5	97	1.62	3
60		12 : 03	2.2	92	(0.8)	1
61		13 : 04	2.2	90	(0.6)	1

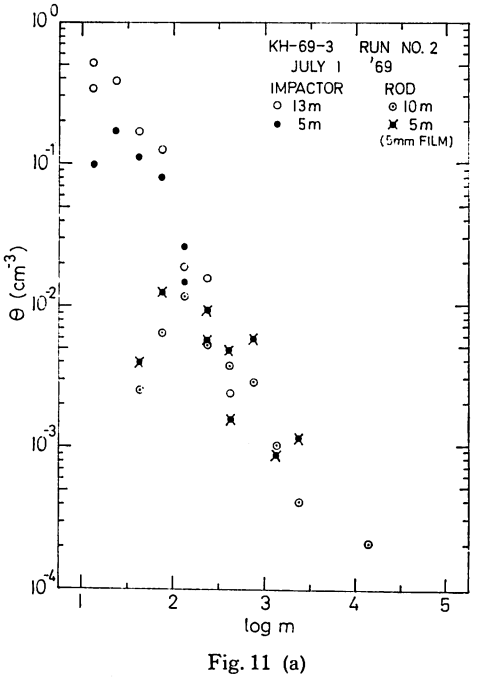

Fig. 11 (a)

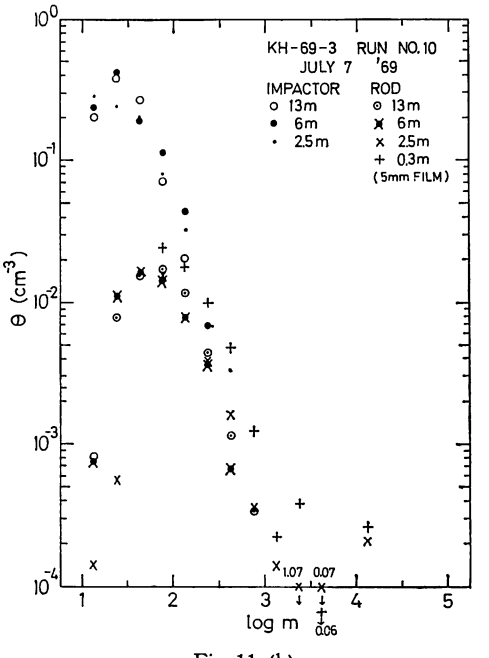

Fig. 11 (b)

Fig. 11. Some examples of the salt-mass distribution of the number concentration of sea-salt particles obtained on board the Hakuhō Maru, (a) Run No. 2, (b) No. 10, (c) No. 15 in the KH-69-3 Cruise, and (d) Run No. 12, (e) No. 19, (f) No. 31, (g) No. 37, (h) No. 52, (i) No. 53 and (j) No. 60 in the KH-70-3 Cruise. Values are entered for ranges of log $m = 0.25$. Values of θ indicated with an arrow on the bottom of the figuer should be multiplied by 10^{-3}. Data of the wind speed, the relative humidity and wind waves at the time of observation are shown in Table 2.

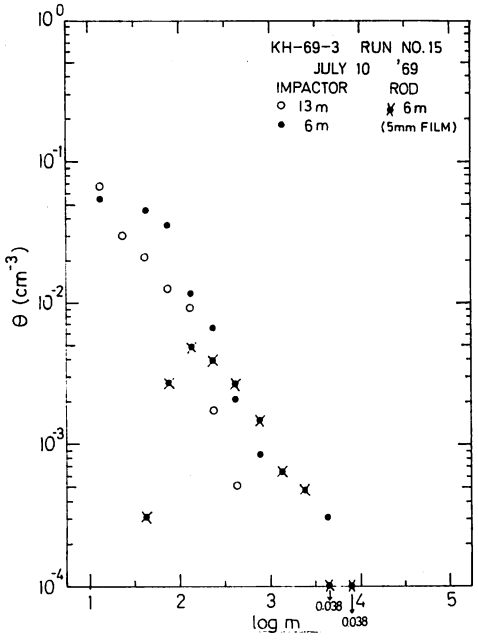

Fig. 11 (c)

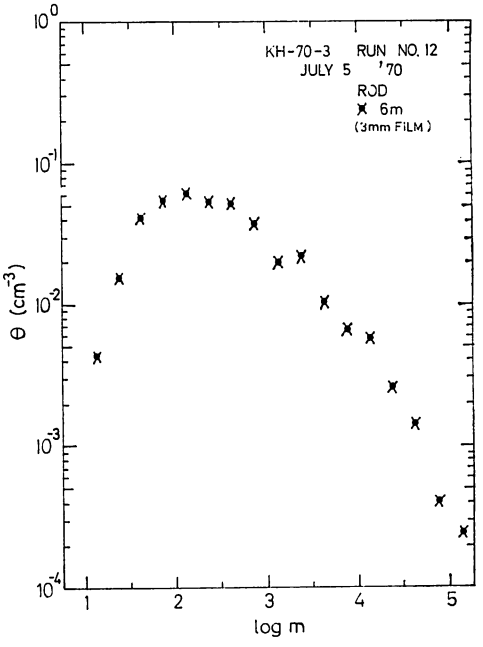

Fig. 11 (d)

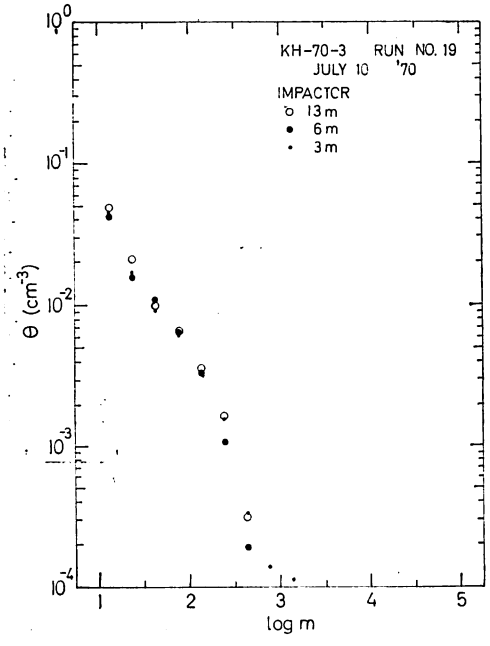

Fig. 11 (e)

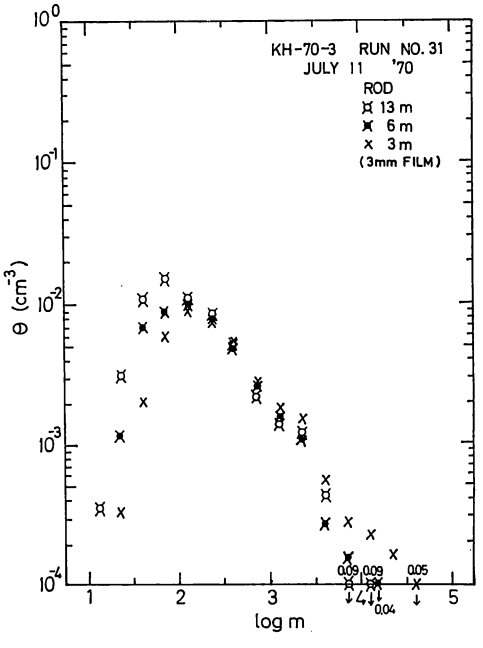

Fig. 11 (f)

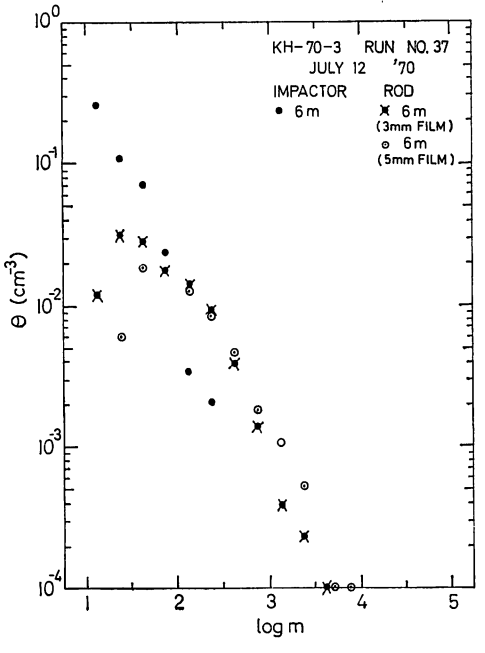

Fig. 11 (g)

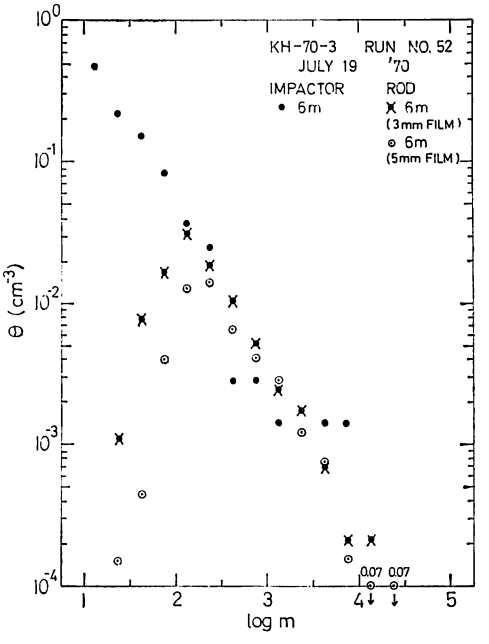

Fig. 11 (h)

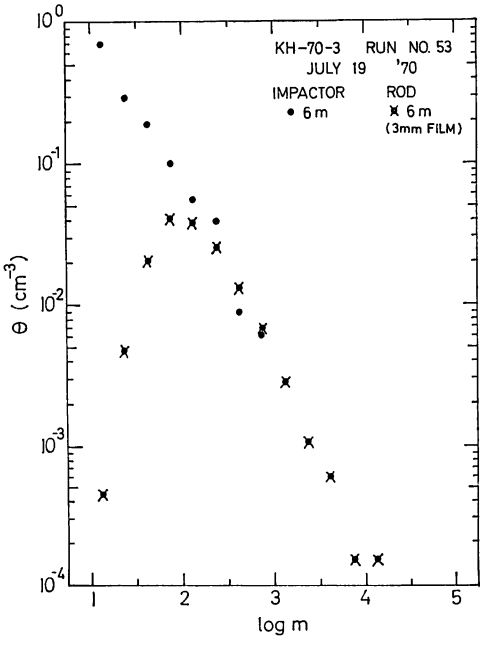

Fig. 11 (i)

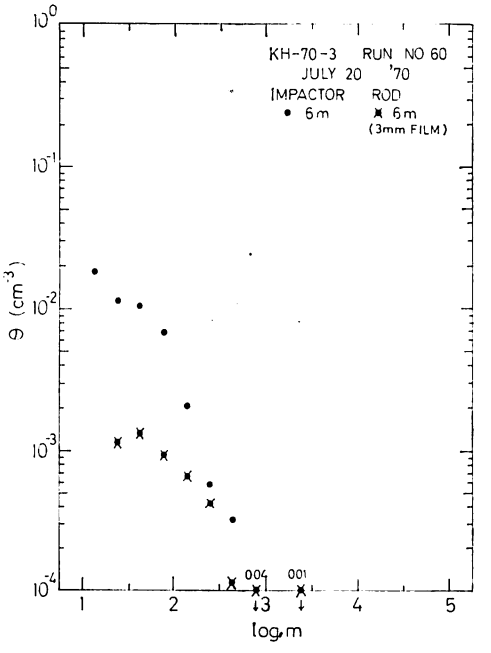

Fig. 11 (j)

2.3. On the efficiency of impaction of sea-salt particles

For the use of the impactor, two kinds of correction should be considered, one is the efficiency of impaction of the impactor, and the other is the retention factor of particles. Firstly, the efficiency of impaction of the impactor with a round orifice of 1 mm diameter is considered to be 100% for giant sea-salt particles, if the syringe is drawn at a speed of 3 sec per 100 cc or faster, as mentioned in section 2. 1. 1. Secondly, the retention factor of particles is the ratio of the collected particle number to that impinged on the sampling surface. This means that there is a possibility that particles once collected on the sampling surface may be blown off again by the air jet. Toba and Tanaka (1967) found that counted particle number is not twofold for a twofold sampled volume of air, by the experiments for various volumes of air, and it named the retention factor. The value of the retention factor sharply changes for small sampled volumes of air and becomes 0. 3 to 0. 25 for very large ones.

In the Hakuhō Maru cruises, the retention factors were obtained from the observations for various sampled volumes of air. The values in the KH-69-3 and KH-70-3 cruises are shown in Table 3, together with the values obtained by Toba and Tanaka (1967) and Tanaka (1970, 1971). The values obtained in the two cruises are almost same, and they are close to the values of Toba and Tanaka (1967). Tanaka's values are smaller than those of the Hakuhō Maru observation by about 0. 1 in each sampled volume of air. It is considered that the sea-salt particles in the observation by Tanaka were drier than in the case of the present observation, because

Table 3. Values of retention factor.

Sampled volume of air (l)	0.1	0.2	0.5	1	2	4	8
Values for KH-69-3 obs.	0.95	0.85	0.66	0.55	0.45		
Values for KH-70-3 obs.	0.90	0.81	0.72	0.63	0.54	0.45	
Values by Toba and Tanaka (1967)	0.92	0.85	0.69	0.54	0.41	0.33	0.29
Values by Tanaka (1970)	0.83	0.73	0.56	0.42	0.35	0.31	
Values by Tanaka (1971)	0.79		0.43	0.30	0.24	0.20	

Tanaka's observations were carried out on the ground near shore. The number concentration of sea-salt partilces by the impactor was corrected by use of the retention factor for each cruise, respectively.

The efficiency of impaction of film ribbon had been studied by Langmuir and Blodgett (1946) and Ranz and Wong (1952) on the bases of experiments and theoretical considerations. Ranz and Wong showed the efficiency of impaction of aerosol particles, for various cases such as rectangular and round aerosol jet with width or diameter Dj against the flat plate, and the efficiency of impaction of disk and ribbon with width or diameter Dj (two-dimensional model of a sphere and of a cylinder, respectively) placed in aerosol streams. These results were presented in graphical forms, where the efficiency of impaction was plotted as a function of the dimensionless parameter expressed by

$$\sqrt{\psi} = (C\rho_p U/18\mu Dj)^{\frac{1}{2}} Dp \qquad (2.1)$$

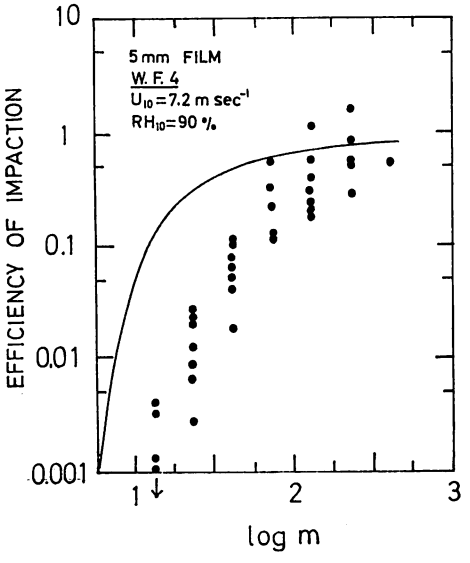

Fig. 12 (a)

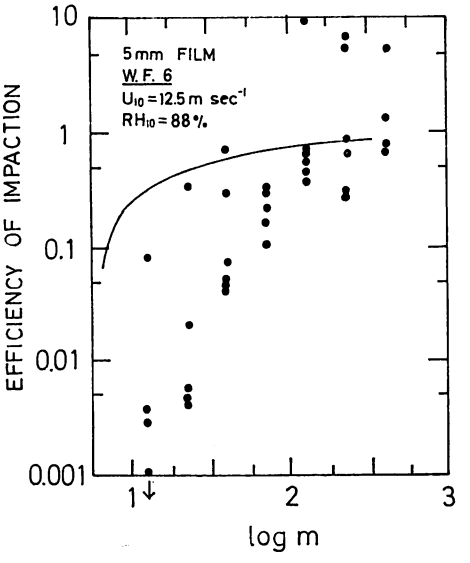

Fig. 12 (b)

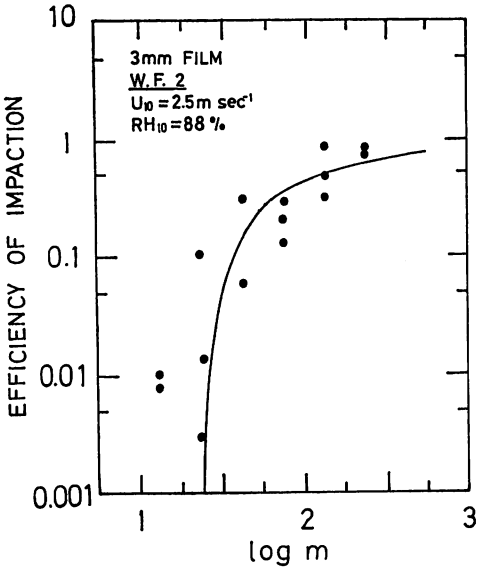

Fig. 12 (c)

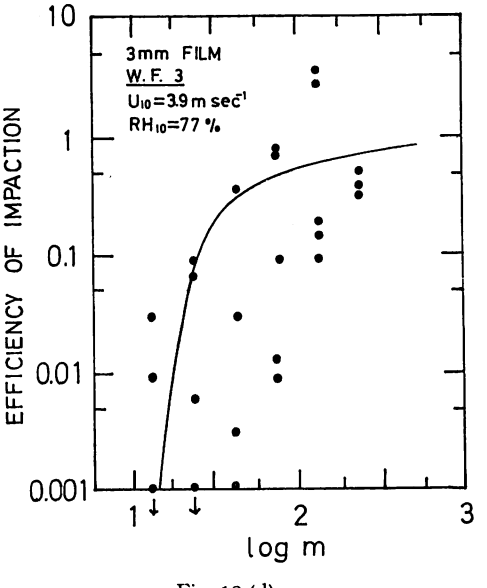

Fig. 12 (d)

Fig. 12. Efficiency of impaction of sea-salt particles for various salt-mass classes by the rod sampler using 5-mm and 3-mm wide films, and for each wind force : (a) 5 mm, W. F. 4, (b) 5 mm, W. F. 6, (c) 3 mm, W. F. 2, (d) 3 mm, W. F. 3, (e) 3 mm, W. F. 4, and (f) 3 mm, W. F. 5. Solid curve indicates the theoretical efficiency of impaction calculated from equation (2. 1) by Ranz and Wong (1952).

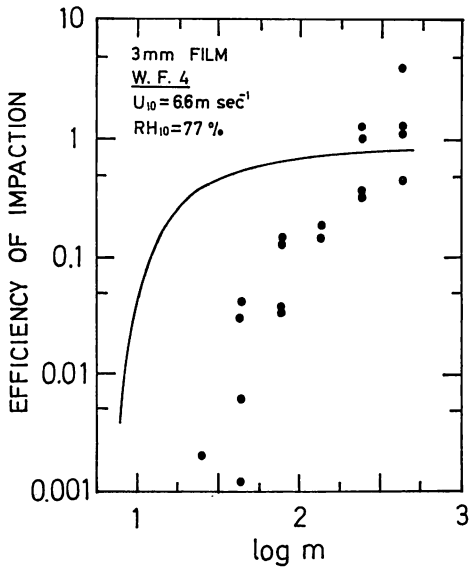

Fig. 12 (e)

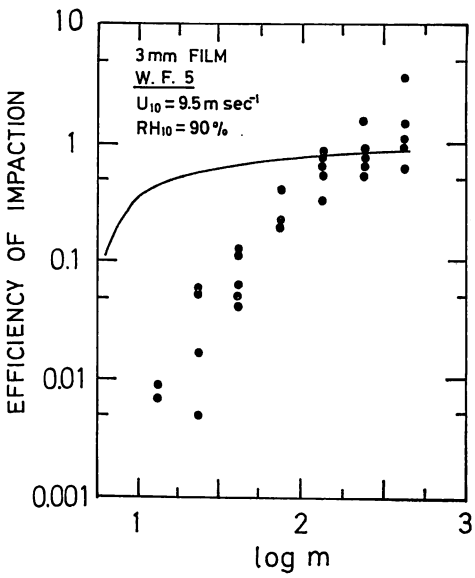

Fig. 12 (f)

where, ρ_p and Dp was the particle density and the diameter, respectively, U the velocity of uniform air flow or jet, μ the viscosity of air, which were all expressed in the c.g.s. unit. The $\sqrt{\psi}$ is a quantity which is proportional to the particle diameter, Dp, when $C = 1$, namely, $(CU/18\mu Dj)^{\frac{1}{2}}$ = constant for a certain collector under a specific air flow, and the ρ_p takes respective values at the conditions of the relative humidity under consideration.

In the Hakuhō Maru cruises, the efficiency of impaction of the rod sampler was obtained as the ratio of the particle number by the rod sampler to that by the impactor, from the simultaneous observations. The efficiency of impaction for each class of the salt mass is shown in Fig. 12, which is presented for each wind force. The solid curve in the figure represents the theoretical efficiency of impaction under the condition of the mean wind speed and the mean relative humidity at the time of observation, calculated from equation (2. 1). The observed efficiency of impaction coincides with the theoretical one, when the wind speed was weak as 2 or 3 m sec^{-1}. In the case of wind speed larger than 5m sec^{-1}, both are not in agreement for the salt-mass class of about $\log m \leqq 2$, namely, the observed efficiency of impaction is low compared with the theoretical one. However, in the salt-mass class of $\log m \geqq 2.25$, the efficiency of impaction for the 3 mm wide film is almost 90%, and for the 5 mm wide film, it is a little lower compared with that of the 3 mm wide one. Naturally speaking, 3 mm wide film is more reliable than 5 mm one, in the efficiency of impaction, as also shown in Fig. 13.

The efficiency of impactions of 5 mm and 3 mm wide films, for salt-mass classes of $\log m \leqq 2.5$, are plotted against $\sqrt{\psi}$, respectively (Fig. 14. a, b). The figures show a large scattering of points. Consequently, it is concluded from the data obtained in the present observation that to apply, without consideration, the normalized equation (2. 1) by Ranz and Wong is unsuitable. The fact that the observed values of efficiency of impaction scatter largely compared with the experimental results by Ranz and Wong may be caused by the results of the field observation under the turbulent air flows.

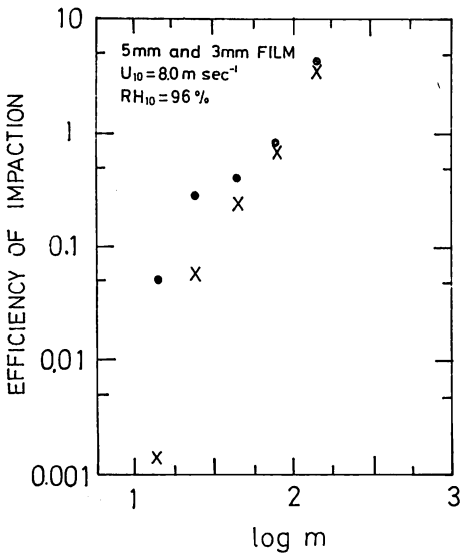

Fig. 13 (a)

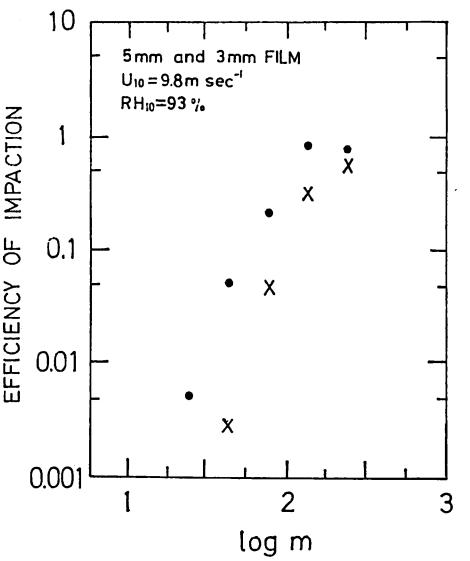

Fig. 13 (b)

Fig. 13. Efficiency of impaction of sea-salt particles for various salt-mass classes by the rod samplers using 5-mm and 3-mm wide films of the simultaneous observations. Crosses and dots indicate 5-mm and 3-mm wide film, respectively.

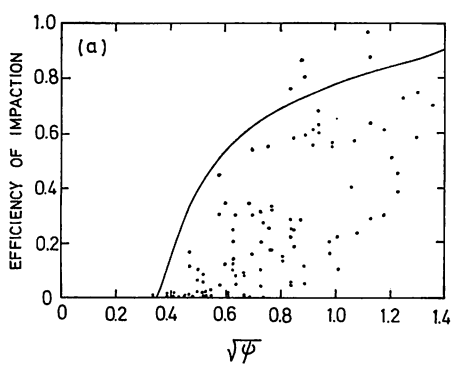

Fig. 14 (a)

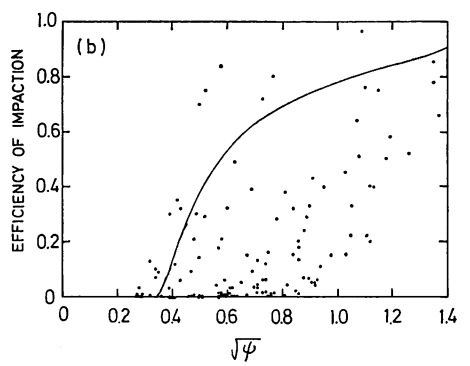

Fig. 14 (b)

Fig. 14. Normalized efficiency of impaction of sea-salt particles for the salt-mass class of log $m \leqq 2.5$ by the rod sampler, (a) 5-mm wide film and (b) 3-mm one. Solid curve indicates the theoretical efficiency of impaction by Ranz and Wong (1952).

3. Vertical distribution of sea-salt particles in the lowest atmospheric layer above the sea surface

3.1. Toba's theory concerning the vertical distribution of sea-salt particles

As to the theoretical study on the vertical distribution of sea-salt particles in the lowest atmospheric layer above the sea surface, there is only one theory of the equilibrium distribution by Toba (1965a). After sea-salt particles are produced on the sea surface, they are suspended in the atmospheric layer above the sea surface, by the balance between falling due to the grav-

itational force and the eddy diffusion. While a sea-salt particle is suspended in the form of a droplet in the air, it has the equilibrium vapor pressure for a solution of the salinity of that droplet. If the vapor pressure surrounding the droplet is smaller than the equilibrium vapor pressure on the droplet, the size of droplet becomes small and the density of saline solution becomes large due to evaporation. In the contrary case of the condition of vapor pressure, the size of the droplet becomes large and the density of solution becomes small through condensation. The equilibrium relative humidity for a droplet of saturated salt solution is about 75%.

Toba's theory (1965 a) is summarized as follows. The vertical distributions of wind speed, vapor pressure and temperature obey a logarithmic law. He considered a case where a steady state holds with no horizontal gradient, but the fall velocity by the gravitational force, w, of sea-salt particles as well as the eddy diffusivity, D, change with the height, z. Although the fall velocity varies in a complicated way from droplet to droplet, for simplicity, each droplet instantly attains its equilibrium salinity for the vapor pressure and temperature of the surrounding air, and the vapor pressure and temperature are given as functions of z. Consequently, the terminal velocity is a function of z, if the mass of salt is given. Now, the equation of diffusion of the number concentration of sea-salt particles, θ, is written as follows

$$\frac{d}{dz}(w\theta)+\frac{d}{dz}\left(D\frac{d\theta}{dz}\right)=0 \tag{3.1}$$

where the eddy diffusivity is expressed by $D = ku_*(z+z_0)$, and where k is the von Kálmán constant and u_* the friction velocity. For the boundary conditions : $\theta = \theta_0$ at $z = 0$ and $\theta = 0$ at $z = \infty$, the solution of equation (3. 1) is expressed in the following form

$$\log(\theta/\theta_0) = -m^{\frac{2}{3}}U_{10}^{-1}\chi\,(RH_{10},\ \gamma_{10},\ z) \tag{3.2}$$

In this expression, the logarithm of the ratio θ to θ_0 is expressed as being proportional to the

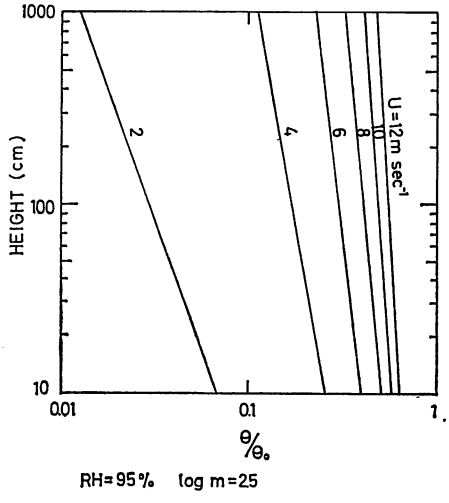

Fig. 15. Theoretical vertical distribution of sea-salt particles of $\log m = 2.5$, calculated from equation (3. 2) by Toba (1965a) for the condition of $RH_{10} = 95\%$.

two thirds power of salt mass contained in a particle, m, and inversely proportional to the wind speed at the 10-m level, U_{10}, with a factor χ which is a function of the relative humidity at the 10-m level, RH_{10}, the friction coefficient, γ_{10}^2 and the height, z. Since the value of γ_{10}^2 does not vary largely in the wind speed range from three or four to ten and odd m sec^{-1}, and is about 1.6×10^{-3}, the value of χ at a height of 10 m is regarded as a function of RH_{10} only. Consequently, the value of θ/θ_0 is expressed as the function of m, U_{10} and RH_{10}. In conclusion, the vertical distribution of the number concentration for each class interval of mass of salt, θ, is along a straight line on a logarithmic diagram of $\log z$–$\log \theta$.

According to this theory, the higher the relative humidity and the weaker the wind speed, the more the particle number concentration decreases with height, on the other hand, the lower the relative humidity and the stronger the wind speed, the more the particle number concentration is distributed nearly uniformly in the 10-m layer over the ocean. Fig. 15 shows the theoretical vertical distribution for the class of salt mass of $\log m = 2.5$ under $RH_{10} = 95\%$, the value of θ/θ_0 being calculated from equation (3. 2).

As to the confirmation Toba's theory from the results of observation, there are two significant points, one is the shape of the distribution on the $\log z$–$\log \theta$ diagram and the other is its vertical gradient. To compare the observed gradient with the theoretical one for a given RH (%) means to check the assumption that the sea-salt particles instantaneously attain their equilibrium salinities for the environmental air at their momentary height.

3.2. Observed vertical distribution of sea-salt particles

The situation of the vertical distribution of the number concentration of sea-salt particles is now examined on the basis of much data. The observations of vertical distribution were carried out at 3 or 4 levels above the sea surface on board ships, as already described. At the anchored station in the East China Sea, the hourly observation for two days was carried out, under weak

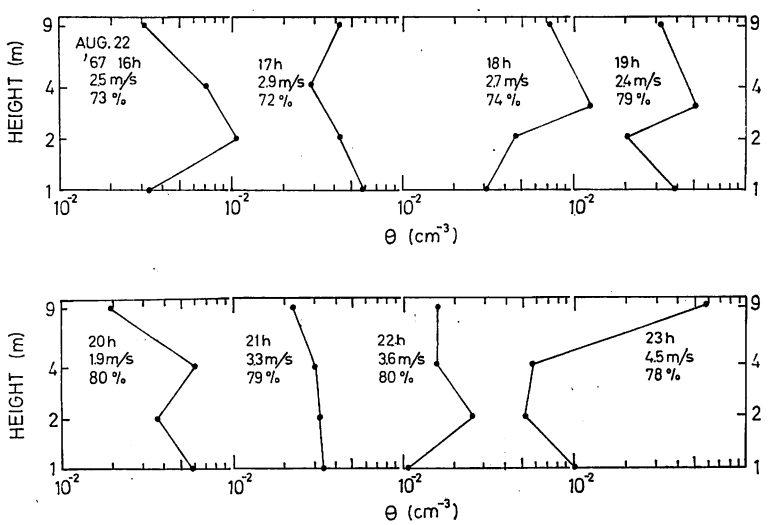

Fig. 16. Some examples of hourly observed vertical distribution of sea-salt particles for two days from 16:00 Aug. 22 to 15:00 Aug. 24 in 1967 at the anchored station in the East China Sea.

wind conditions of 1.9～5.8 m sec^{-1} and a mean relative humidity of 77%. Some of these results are shown in Fig. 16. The shape of the vertical distribution of sea salt-particles every hour has various types. The values of θ for a class of $\log m = 1.28$～2.53 at each level are distributed in a wide range of 5×10^{-3}～1×10^{-1} cm^{-3}, but the mean vertical distribution of θ is very close to a straight line on the logarithmic diagram as shown in Fig. 17. The same tendency

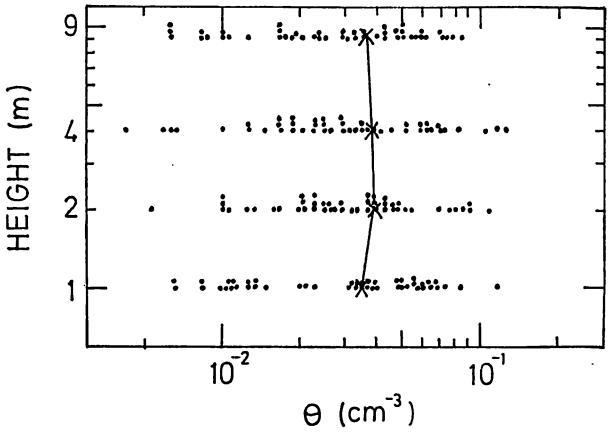

Fig. 17. Hourly observed vertical distributions of sea-salt particles (dots) of 48 times for two days and their mean vertical distribution (solid line with crosses).

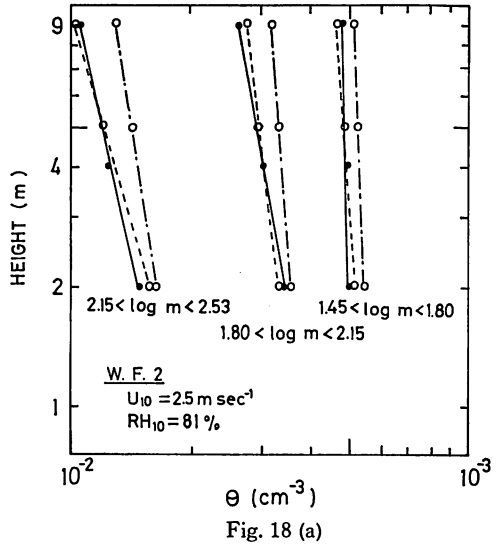

Fig. 18 (a)

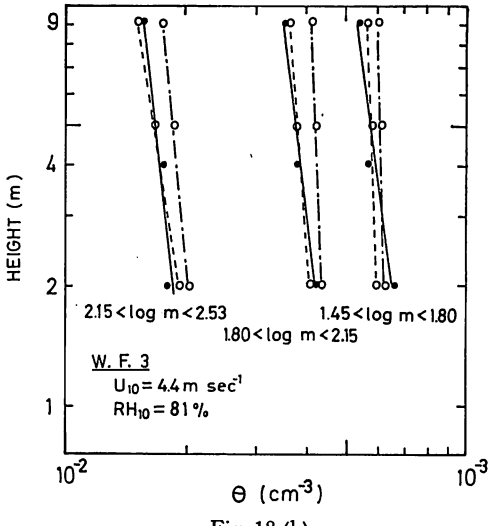

Fig. 18 (b)

Fig. 18. Mean observed vertical distribution of sea-salt particles (black circles) obtained on board the Kagoshima Maru in the Indian Ocean, (a) in wind force 2, (b) wind force 3, (c) wind force 4 and (d) wind force 5. Dashed and dash-dot lines with circles indicate the theoretical vertical distributions by Toba's model for the conditions of $RH_{10} = 95\%$ and mean RH_{10} at the time of observation in each wind force, respectively. The abscissa is θ/θ_0 in the theoretical model. They are entered at near the observed one, for the comparision of the vertical gradient.

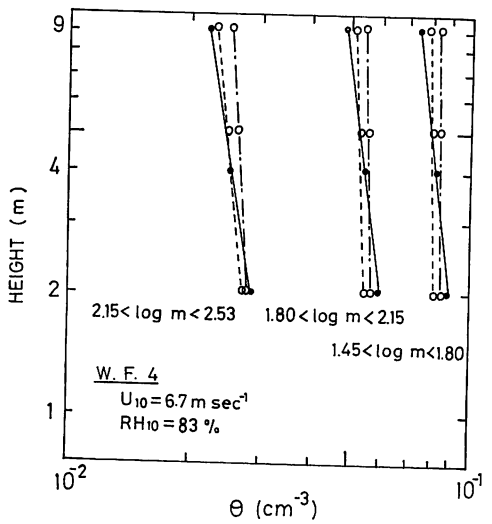

Fig. 18 (c)

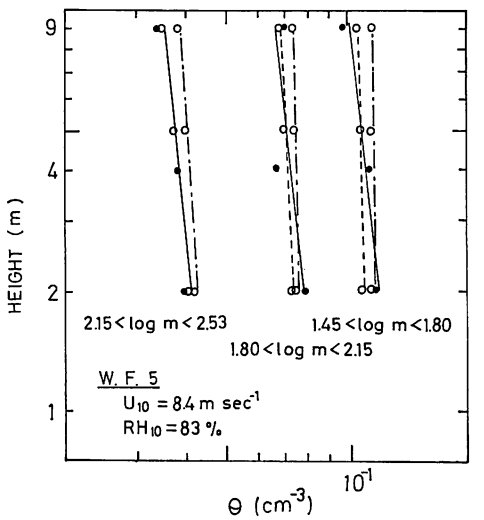

Fig. 18 (d)

is also found in the vertical distributions of physical quantities, such as wind speed and vapor pressure above the sea surface. These show straight lines on an average on a semi-logarithmic diagram, though individual distributions have various shapes.

In the case of the observation of sea-salt particles, the complicated shape of vertical distribution seems to be caused by the fact that the time required for one observation of vertical distri-

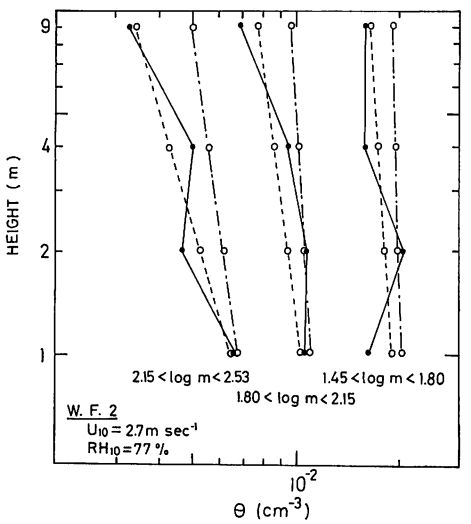

Fig. 19 (a)

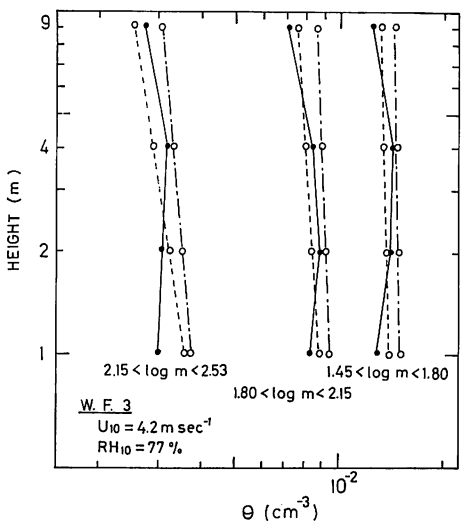

Fig. 19 (b)

Fig. 19. Mean observed vertical distribution of sea-salt particles (black circles) obtained on board the Kagoshima Maru in the East China Sea, (a) in wind force 2 and (b) wind force 3. Dashed and dash-dot lines with circles indicate the theoretical vertical distributions by Toba's model for the conditions of $RH_{10} = 95\%$ and mean RH_{10} at the time of observation in each wind force, respectively. The abscissa is θ/θ_0 in the theoretical model. They are entered at near the observed one, for the comparision of the vertical gradient.

bution was short, ranging from about 3 to several minutes in the Kagoshima Maru Cruise and about 20 sec to 1 minute in the Hakuhō Maru Cruise. In other wards, this may be a rather natural condition in the turbulent air flows. In Fig. 18 and 19 is presented the mean vertical distribution of sea-salt particles for various wind forces, observed in the Indian Ocean, and in the East China Sea, respectively. They are shown for the three classes of salt mass, i.e., $1.45 < \log m < 1.80$, $1.80 < \log m < 2.15$, and $2.15 < \log m < 2.53$, and for each wind force. The numbers of observations of the vertical distribution of sea-salt particles in the Indian Ocean are 29, 30, 32 and 20 in wind force 2, 3, 4 and 5 respectively, and those in the East China Sea are 20 and 33 in wind force 2 and 3, respectively. The mean wind speed at the 10-m level and the mean relative humidity for each wind force are shown in the figures. It is seen in the figures that the mean vertical distribution of the number concentration of sea-salt particles is very close to a straight line on the logarithmic diagram. From these results, it may be considered that one of the significant points of Toba's theory is substantiated.

3.3 Observed vertical gradient of the distribution

For inspecting the other point of the theory, theoretical vertical distributions calculated from equation (3.2) for the conditions of the mean relative humidity, and the mean wind speed for each observation are shown in the figures by dash-dot lines. Theoretical vertical distributions calculated for the conditions of $RH_{10} = 95\%$ are also shown in the figures by dashed lines (Fig. 18 and 19). It is seen that the observed mean vertical gradients become large with increasing salt mass, as predicated by Toba's theory. Comparing the observed vertical gradient with the theoretical one, the former is larger than the latter for the mean relative humidity during the observations, and approximately coincides with the latter for $RH_{10} = 95\%$.

Further, the vertical distribution of θ obtained on board the Hakuhō Maru are shown in Fig. 20, for each class of salt mass, for each wind force, and for each run. In the figures, the two theoretical distributions for the RH_{10} of the observation time and the conditions of $RH_{10} = 95\%$ are also entered. The observed vertical distributions at three heights show various shapes, such as a straight line and a hook shape. In wind force 3, the vertical gradient for the salt-mass class of $\log m \leqq 1.75$ has the inverse gradient, which indicates that many small sea-salt particles produced before the observation exist in the air. It is seen from the figures that the vertical gradient becomes large with the increasing salt masses. In wind force 6, the same situation is also recognized clearly. Comparing the observed gradient with the theoretical one, here also, the observed gradient is larger than the theoretical one for the condition of the mean relative humidity at the observed time, and the former approximately coincides with the latter for the condition of $RH_{10} = 95\%$.

In the results of the observation of the vertical distribution of sea-salt particles at the Shirahama Oceanographic Tower Station by Toba et al. (1971), it was found that the shape of vertical distribution for the salt-mass class of $\log m = 2.25 \sim 2.75$ was nearly a straight line on the logarithmic diagram, and the vertical gradient was close to the theoretical one for the condition of $RH_{10} = 95\%$.

So far, the situation of the vertical distribution of sea-salt particles for each class of salt mass for each wind force were presented, and the comparison of the observed vertical gradient with the theoretical one was tried. Now, the gradient between two heights can be obtained, according

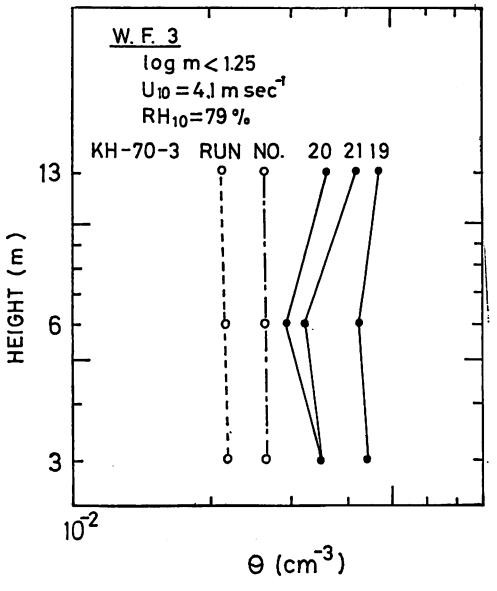

Fig. 20 (a-1)

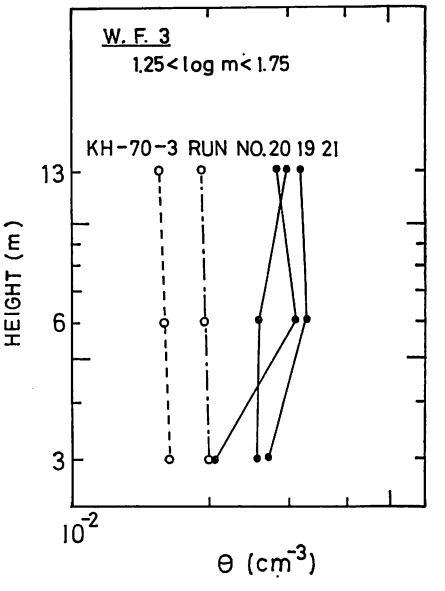

Fig. 20 (a-2)

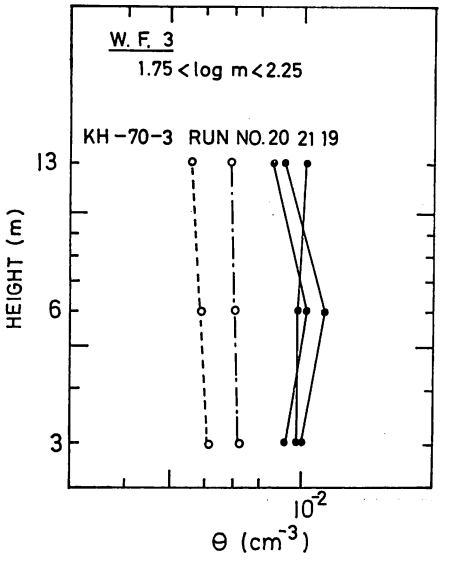

Fig. 20 (a-3)

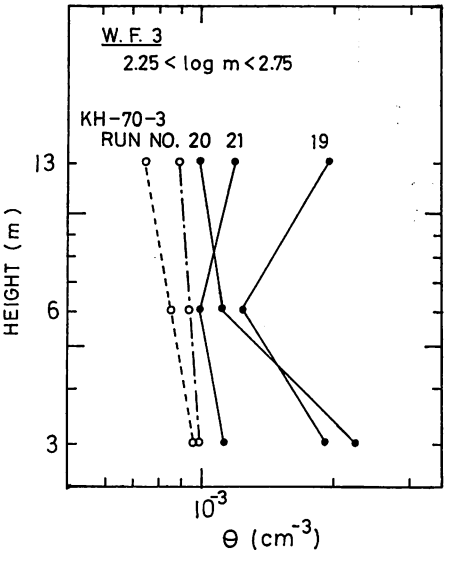

Fig. 20 (a-4)

Fig. 20. Observed vertical distributions of sea-salt particles (black circles) obtained on board the Hakuhō Maru, (a) in wind force 3, (b) wind force 4 and (c) wind force 6. Dashed and dash-dot lines with circles indicate the theoretical vertical distributions by Toba's model for the conditions of $RH_{10} = 95\%$ and mean RH_{10} at the time of observation in each wind force, respectively. The abscissa is θ/θ_0 in the theoretical model. They are entered at near the observed one, for the comparision of the vertical gradient.

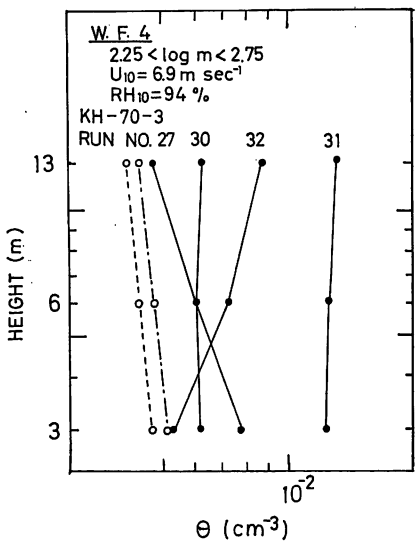

Fig. 20 (b-1)

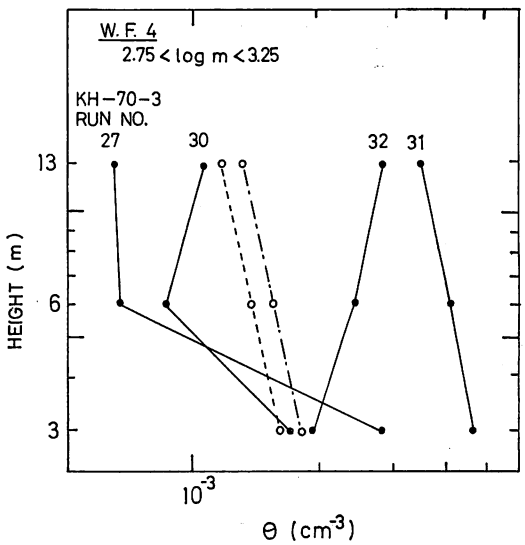

Fig. 20 (b-2)

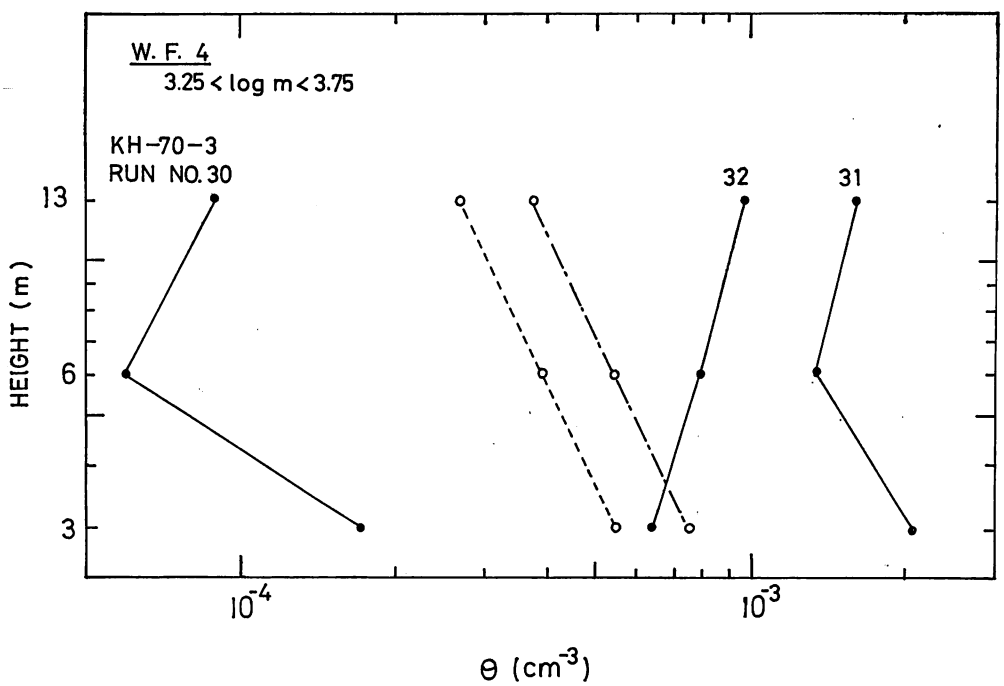

Fig. 20 (b-3)

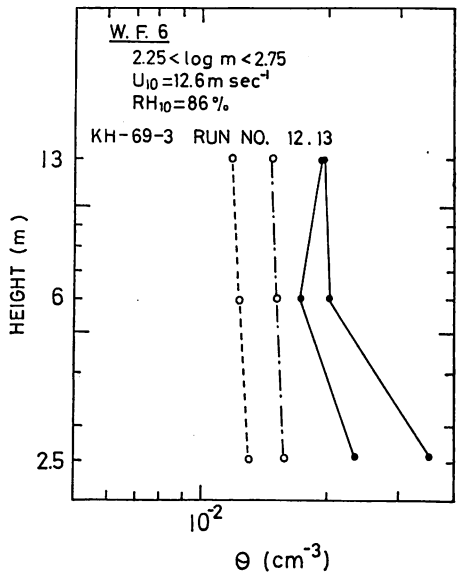

Fig. 20 (c-1)

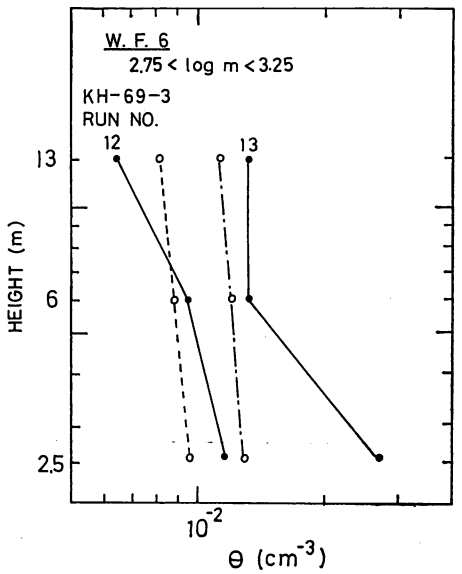

Fig. 20 (c-2)

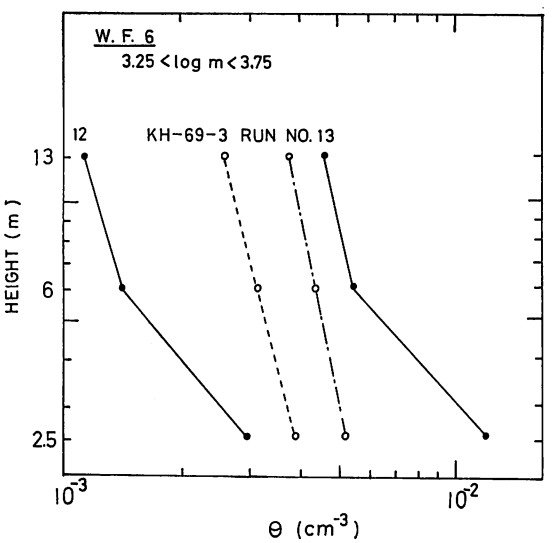

Fig. 20 (c-3)

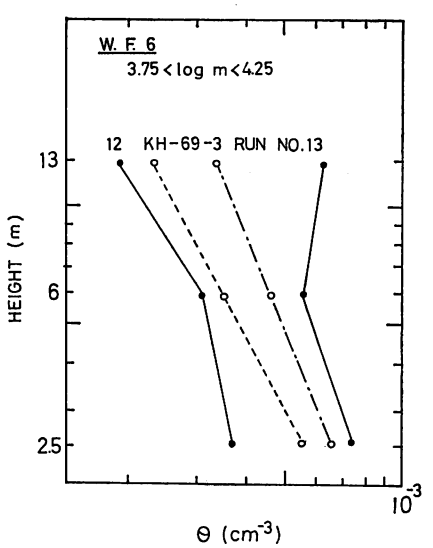

Fig. 20 (c-4)

to equation (3. 2). Namely, if two heights are expressed by z_a and z_b, from equation (3. 2) it follows

$$-(\log \theta z_a/\theta_0 - \log \theta z_b/\theta_0) = (\chi z_a - \chi z_b) m^{\frac{2}{3}} U_{10}^{-1} \tag{3.3}$$

The θ_0 is unknown, and the left side of equation (3. 3) is expressed by, $\log \theta z_a - \log \theta z_b$. The gradient, G, between the two heights, z_a and z_b is as follows:

$$G = \frac{\log \theta z_b - \log \theta z_a}{\log z_a - \log z_b} \tag{3.4}$$

Values of G are plotted against $m^{\frac{2}{3}} U_{10}^{-1}$ at the time of observation, as shown in Fig. 21. In the results of the KH-69-3 and KH-70-3 cruises, values of G for the salt-mass class of $\log m \leqq 2.5$ by the rod sampler and for that of $\log m \geqq 2.5$ by the impactor are excepted from the plotting,

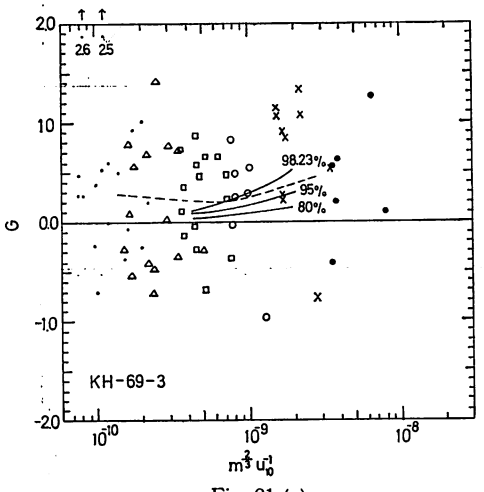

Fig. 21 (a)

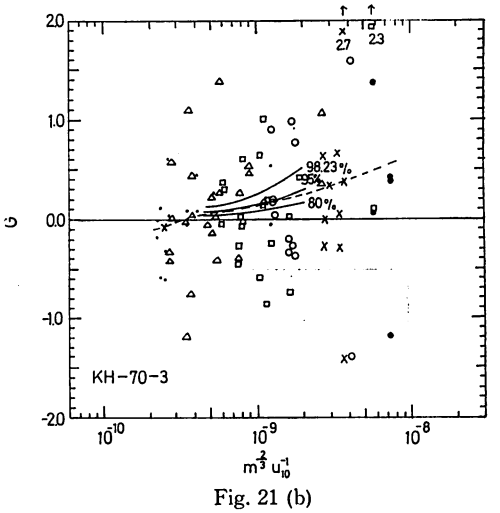

Fig. 21 (b)

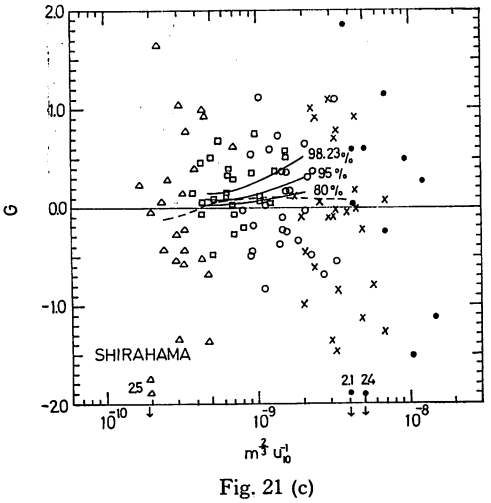

Fig. 21 (c)

Fig. 21. Values of the gradient between two heights, G, plotted against the values of $m^{\frac{2}{3}} U_{10}^{-1}$ at the time of observation, (a) in the KH-69-3, (b) KH-70-3 cruises and (c) at the Shirahama Oceanographic Tower Station. Values are entered for ranges of $\log m = 0.5$. Symbols of salt-mass class: dots, $\log m = 1.25 \sim 1.75$; triangles, $\log m = 1.75 \sim 2.25$; squares, $\log m = 2.25 \sim 2.75$; circles, $\log m = 2.75 \sim 3.25$; crosses $\log m = 3.25 \sim 3.75$; and solid circles, $\log m = 3.75 \sim 4.25$. Dashed line indicates the mean gradient of G. Solid line indicates the theoretical gradient for the condition of $RH_{10} = 98.2\%$, 95%, and 80%, respectively.

because of the low efficiency of impaction. The solid curves in the figure are the theoretical gradients calculated from equation (3.2) for the condition of RH_{10} of 80%, 95% and 98.23% resp-ectively. As shown in the figures, values of G scatter largely at both sides of $G = 0$. This is easily expected from the situation of vertical distribution of sea-salt particles described before. In order to obtain the mean distribution of G against $m^{\frac{2}{3}} U_{10}^{-1}$, values of G are averaged for the ranges of $m^{\frac{2}{3}} U_{10}^{-1}$, such as $1\times10^{-10} \sim 2\times10^{-10}$, $2\times10^{-10} \sim 3\times10^{-10}$, $3\times10^{-10} \sim 5\times10^{-10}$, $5\times10^{-10} \sim 1\times10^{-9}$, $1\times10^{-9} \sim 2\times10^{-9}$, $2\times10^{-9} \sim 4\times10^{-9}$ and larger than 4×10^{-9}. The distribution of mean value of G against $m^{\frac{2}{3}} U_{10}^{-1}$ is found in the middle part of the theoretical distributions of RH_{10} of 95% and 98.2% in the results of KH-69-3, and it nearly coincides with the theoretical one of RH_{10} of 95% in the results of KH-70-3. It is seen that the mean value of G increases with $m^{\frac{2}{3}} U_{10}^{-1}$. The mean relative humidity in the observation of vertical distribution under consideration in Fig. 21 was 92% and 90% in the KH-63-3 and KH-70-3 cruises, respectively. The mean value of G against $m^{\frac{2}{3}} U_{10}^{-1}$ in the results of observation at the Shirahama Oceanographic Tower Station is found at the middle point between the theoretical curves of RH_{10} of 80% and 95%.

From the above-mentioned results, it can be recognized that the observed vertical gradient of the distribution of sea-salt particles in the lowest atmospheric layer above the sea surface, on an average, was close to the gradient calculated from Toba's theory for the condition of $RH_{10} = 95\%$, though the actual RH_{10} at the time of observation was lower than 95%. The fact that the observed gradient coincides with the theoretical one for the condition of the larger relative humidity, leads to the physical explanation that the concentration of the sea-salt solution of each particle is still low, and it is not in equilibrium with the relative humidity surrounding the particle, because many of the sea-salt particles has not been in the air for a long time after produced at the sea surface. As the value of the larger relative humidity, the appropriate value of about 95% has been empirically obtained as discussed above. This apparent larger relative humidity of 95% is named the effective relative humidity.

There is an evidence that supports the empirical value of the effective relative humidity. That is the result of the simultaneous observation by means of two methods of the reagent film and the MgO surface, which is shown in Fig. 22. As shown in the figure, the salt-mass distributions obtained from the two kinds of sampling surfaces do not meet each other for the class of $\log m = 1.5 \sim 3.5$. The salt-mass distribution obtained from the MgO surface is calculated from the drop-size distribution, assuming that the concentration of the sea-salt solution of droplet is in equilibrium with the relative humidity of 98.2% (concentration of sea-salt solution = 35‰). The observed relative humidity was 90%. If the relative humidity is lower than 98.2%, the sea-salt solution is more concentrated, and the calculated salt mass, m, becomes larger. Therefore, the salt-mass distribution obtained from the MgO surface should move to the right on the figure. Assuming that the value of relative humidity at 10-m level is 95%, the salt mass, m, is 2.7 times larger than that for $RH_{10} = 98.2\%$, namely, it should move to the right by $\log m = 0.4$. The difference between the two distributions is about 0.5 in $\log m$. If we make the salt-mass distribution obtained from the MgO surface coincide with that observed by the reagent film, the effective relative humiditiy is to be 94%. For the relative humidity of 90% at the time of observation, the salt mass, m, is calculated to be about 4.8 times

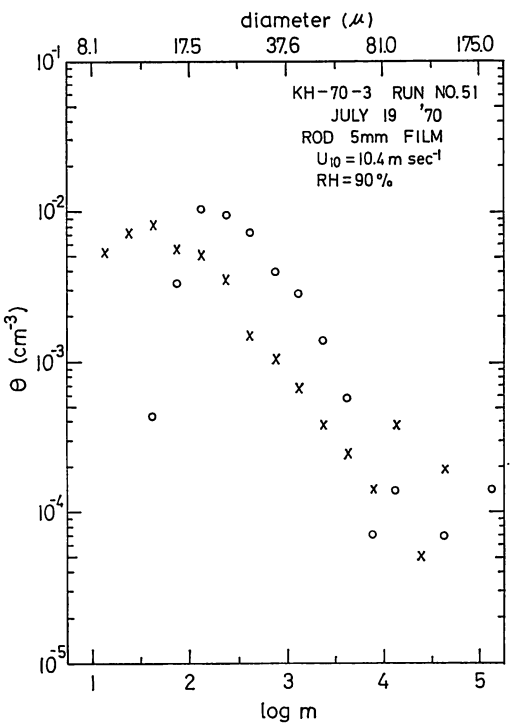

Fig. 22. Salt-mass distributions of the number concentration of sea-salt particles observed by the reagent film (circles) and calculated from the drop-size distribution simultaneously observed by the MgO surface (crosses), by assuming RH of 98.2%.

larger than that of $RH_{10} = 98.2\%$, namely, the distribution curve should move to the right by $\log m = 0.7$. The sea-salt particles larger than $\log m = 3.5$ by means of the two methods approximately overlap with each other in the distribution, this seems to show that the larger sea-salt particles are still near to sea-water droplets.

From the above discussion, it may be concluded that the vertical distribution of the number concentration of sea-salt particles in the lowest atmospheric layer above the sea surface has, on an average, a line very close to a straight line on the logarithmic diagram, though the vertical distributions obtained as the result for a short measuring time have various shapes, and the vertical gradient is approximately expressed by the modified equilibrium theory by the use of the effective relative humidity of 95% at 10-m level.

4. Amount of sea-salt particles in the lowest atmospheric layer above the sea surface and their production rates on the sea surface

4.1. Values of number concentration of sea-salt particles on the sea surface

As described in section 2.2.2, the salt-mass distribution of sea-salt particles in the wide range from $\log m = 1$ to $\log m = 5$ has been able to be obtained, by using two kinds of samplers. In Fig. 23 and 24 are shown the salt-mass distribution of θ for the ranges of $\log m = 0.25$ obtained by connecting both the results by the impactor and the rod sampler, for each wind force in the KH-69-3 and KH-70-3 cruises. The data for wind force 7 in the KH-70-3 cruise is the result obtained by the rod sampler only. The salt-mass distribution of θ represented by a dashed

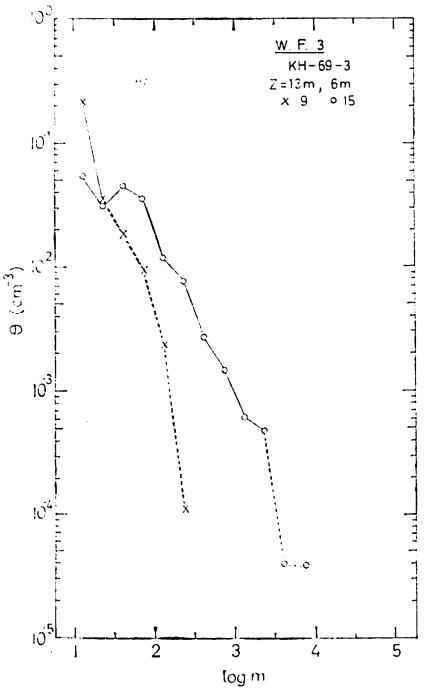

Fig. 23 (a)

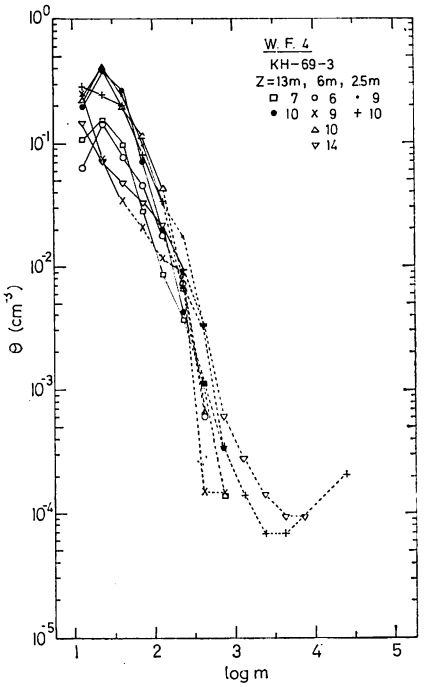

Fig. 23 (b)

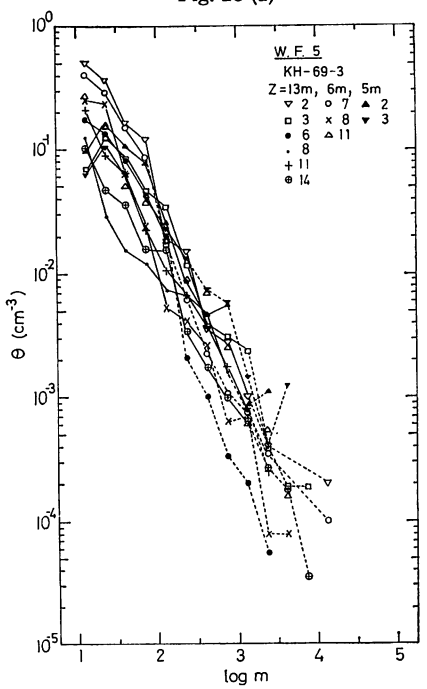

Fig. 23 (c)

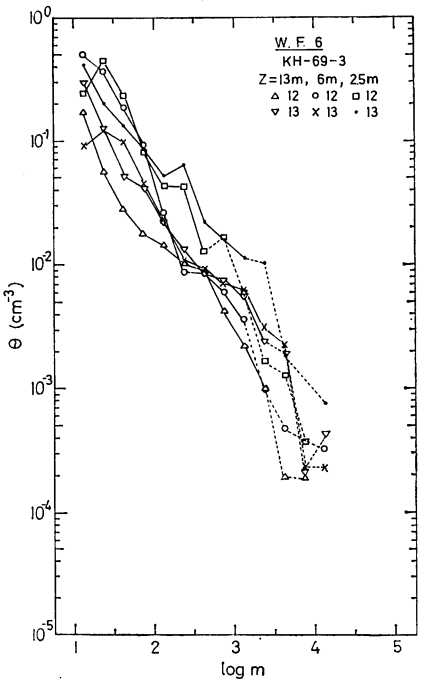

Fig. 23 (d)

Fig. 23. Salt-mass distribution of the number concentration of sea-salt particles, θ, for the ranges of log m = 0.25 obtained by connecting both the results by the impactor and the rod sampler, for each run in the KH-69-3 cruise, (a) in wind force 3, (b) wind force 4, (c) wind force 5 and (d) wind force 6. Symbols and figures indicate the run number.

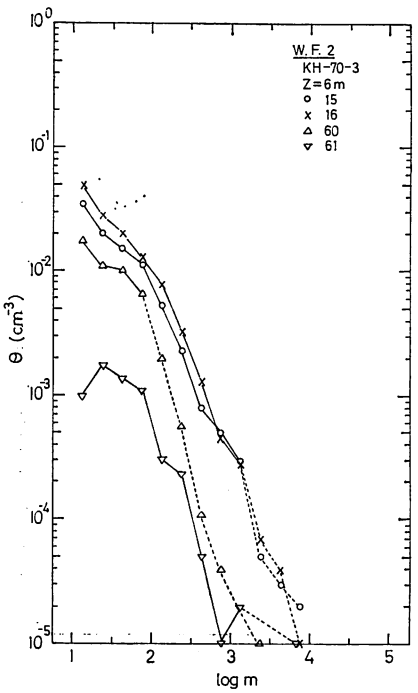

Fig. 24 (a)

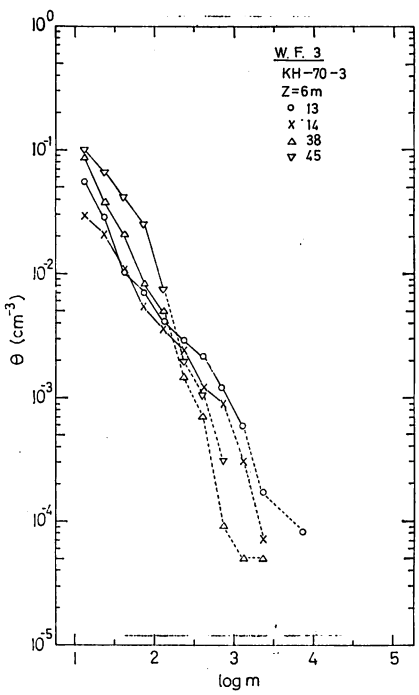

Fig. 24 (b)

Fig. 24. Salt-mass distribution of the number concentration of sea-salt particles, θ, for the ranges of $\log m = 0.25$ obtained by connecting both the results by the impactor and the rod sampler, for each run in the KH-70-3 cruise, (a) in wind force 2, (b) wind force 3, (c) wind force 4, (d) wind force 5, (e) wind force 6 and (f) wind force 7. The data for wind force 7 is the results obtained by the rod sampler only. Symbols and figures indicate the run number.

line is the part where the counted particle number is smaller than ten for each point. It is seen in the figures that θ decreases with increasing $\log m$. Mean salt-mass distribution of θ for each wind force in the two cruises is shown in Fig. 25 and 26, respectively.

In order to compare the values of θ obtained in the KH-69-3 and KH-70-3 cruises with other data, the salt-mass distributions of θ for wind force 5 are shown in Fig. 27. The data used in comparision are the value in the 10-m level over the ocean, derived by Toba (1965), using the data of Woodcock's observation at cloud levels, and the values observed in the sea-surface boundary layer in the Indian Ocean by Chaen (1971) and those at the Shirahama Oceanographic Tower Station by Toba et al. (1971). If we consider the difference of the height of observation, it may be recognized that there is no significant difference among them, with the exception of the value of θ at around $\log m = 3 \sim 3.5$ by Toba (1965). This relatively high value of θ was explained as a result of the coalescence of sea-salt particles which took place during the transport upward from the sea surface by Toba.

In the discussions hereafter, the data obtained in the KH-70-3 cruise will mainly be used, since the observations were carried out in the condition of a relatively wide range from 2 to 7 in wind force compared with that in the KH-69-3 cruise, and since the wind wave data of the peried of significant waves at the time of sampling was obtained. It is seen in Fig. 26 that the feature of the mean salt-mass distribution of θ for each wind force is close to a straight-line seg-

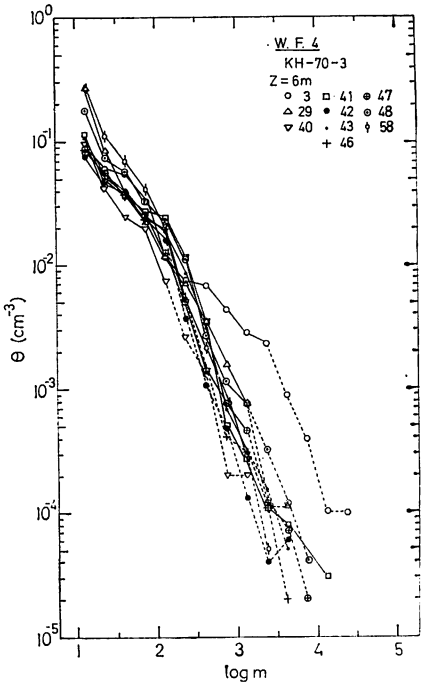

Fig. 24 (c)

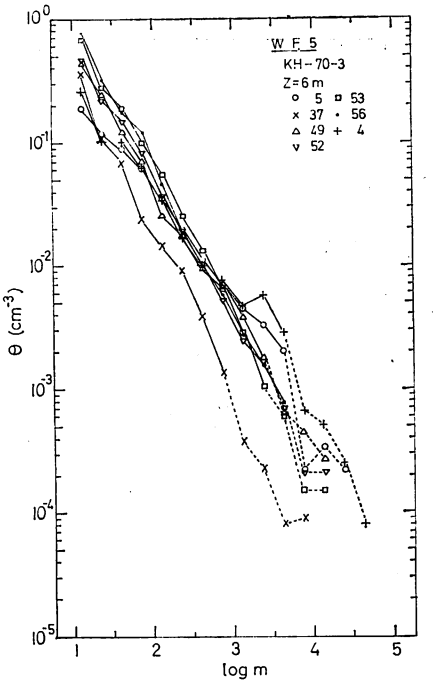

Fig. 24 (d)

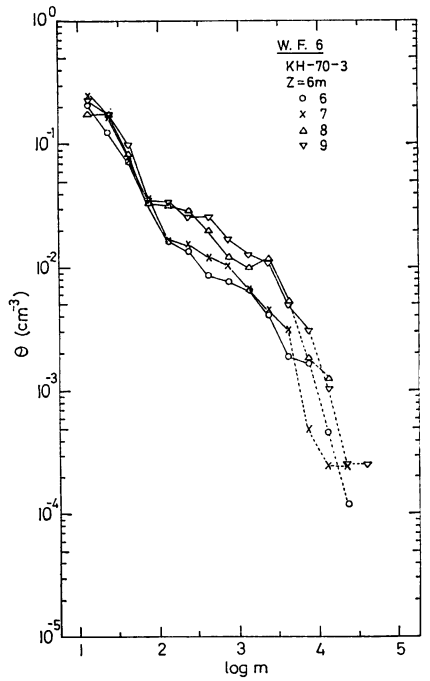

Fig. 24 (e)

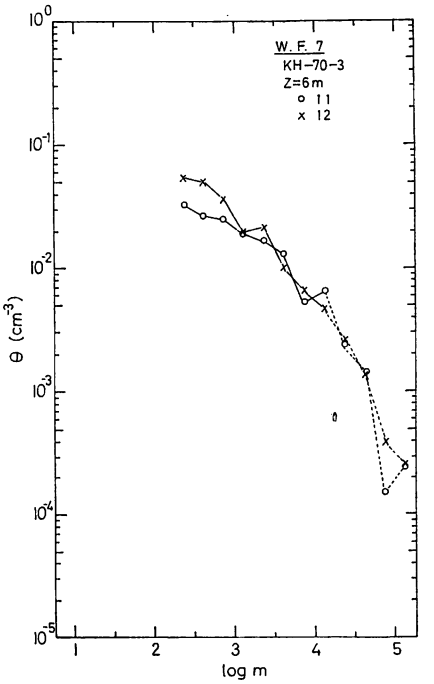

Fig. 24 (f)

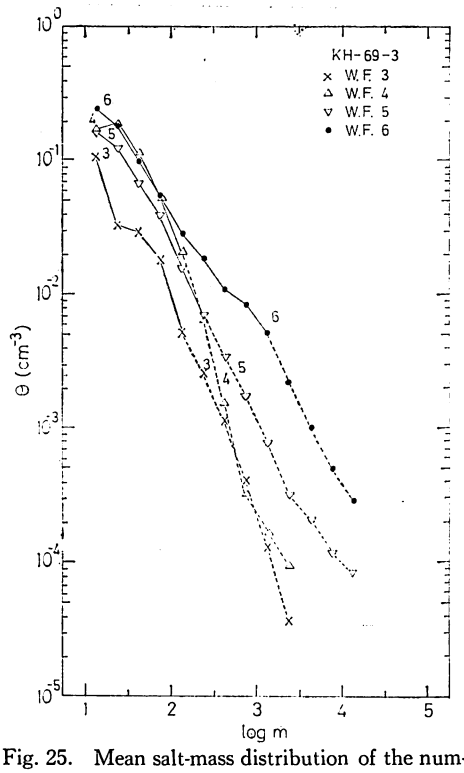

Fig. 25. Mean salt-mass distribution of the number concentration of sea-salt particles, θ, for each wind force for KH-69-3 data (from Fig. 23).

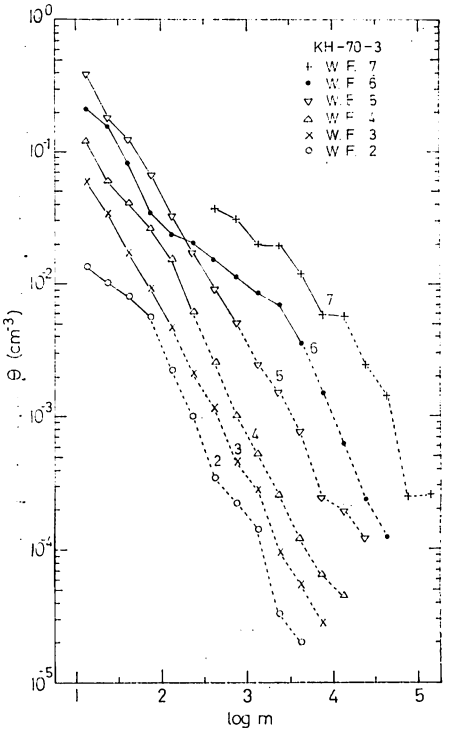

Fig. 26. Mean salt-mass distribution of the number concentration of sea-salt particles, θ, for each wind force for KH-70-3 data (from Fig. 24).

ment, and they are parallel to each other for the salt-mass class of $\log m \leqq 2.25$. In wind force 6, the values of θ for the salt-mass class of $\log m \leqq 2.25$ are low compared with that of wind force 5. This seems to show that the efficiency of impaction of the impactor becomes low for the stronger wind larger than wind force 6.

In connection with the salt-mass distribution of θ mentioned above, there is a well-known relation proposed by Junge (1953, 1958), concerning the number concentration of aerosols, θ, and the radius, r, as expressed by

$$\theta r^3 = \text{constant} \qquad \text{or} \qquad d(\log\theta)/d(\log r) = -3 \tag{4.1}$$

If the radius, r, is replaced by salt mass, m, equation (4.1) is expressed by

$$d(\log\theta)/d(\log m) = -1 \tag{4.2}$$

Namely, it is seen in Fig. 26 that the value of θ take a figure down one place with an increase of $\log m = 1$. The Junge distribution holds very well especially for wind force 5. It is noticeable that the Junge distribution is also applicable to the salt-mass distribution of sea-salt particles in the lowest atmospheric layer above the sea surface.

Now, the value of the number concentration of sea-salt particles at the sea surface must be

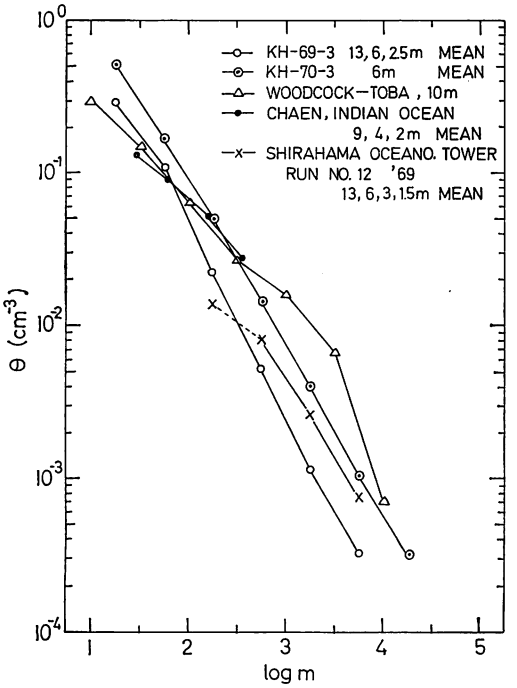

Fig. 27. Salt-mass distribution of the number concentration of sea-salt particles for wind force 5, collected from several sources.

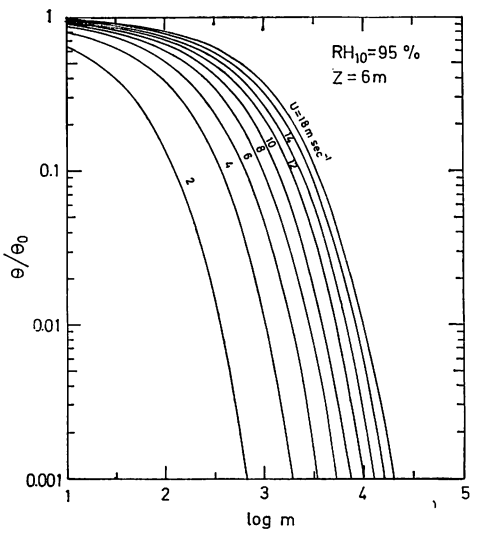

Fig. 28. Predicted ratio of the number concentration of sea-salt particles at 6-m level, θ, to that at $z = z_0$, for the condition of $RH_{10} = 95\%$, by Toba's model.

determined, as a main step in obtaining the production rate of sea-salt particles. However, it is almost impossible to determine the particle number concentration at the sea surface, θ_0, by a direct observation. One of the methods to infer the value at the sea surface will be the use of the observed value at 6 m level above the sea surface, together with the fact that the vertical distribution of sea-salt particles in the lowest atmospheric layer above the sea surface may be represented by the modification of Toba's theory.

The practical procedure for obtaining the value of θ_0 is as follows. Firstly, the relation between, θ/θ_0 and, m, is calculated from equation (3. 2). As an example, the case where height $z = 6$m, the relative humidity at 10-m level $RH_{10} = 95\%$, is shown in Fig. 28. Secondly, the value of θ/θ_0 is read on the graph for each class of salt mass for the wind speeds at 10-m level, U_{10} under consideration, and the value of θ_0 is obtained by multiplying the observed value of θ by θ/θ_0. The value of θ_0 means the particle number concentration at the level of $z = z_0$, the roughness length of the sea surface, as already described by Toba (1965a). From the mean salt-mass distribution of θ for each wind force, obtained from the KH-70-3 cruise (Fig. 26), the values of θ_0 are calculated for the effective $RH_{10} = 95\%$ as shown in Fig. 29. The salt-mass distribution of θ_0 has the lowest value at the class of salt mass of $\log m = 2.5 \sim 2.75$. According to Fig. 29, there is a tendency that the weaker the wind force, the more extreme high value appears for larger m. This tendency was also clearly found in the salt-mass distribution of θ_0 by Toba, (1965a), derived from the data of Woodcock (1953) obtained at cloud base levels. Toba

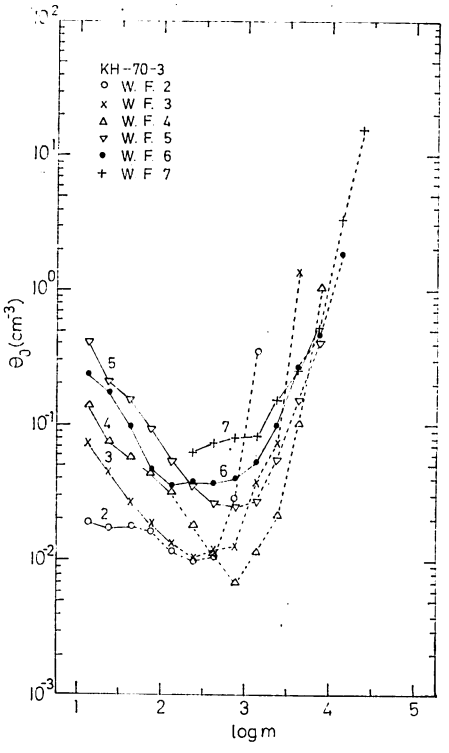

Fig. 29. Values of θ_0 obtained by operating Fig. 28 to Fig. 26.

(1965a) stated that this tendency cannot be accepted as the real situation, and ascribed to the coalescence of sea-salt particles which took place during the transport upward from the sea surface. However, the same tendency is recognized in the shape of the present θ_0 which was obtained from the results of observation in the lowest atmospheric layer above the sea surface. It is unreasonable that larger numbers of sea-salt particles are produced in weak wind speeds than in strong ones. This fact leads to a thought that the tendency was not caused only by the coalescence of particles.

Here, it is unavoidable to reconsider the meaning of θ_0. As will be discussed in the next section, when the value of θ_0 is plotted as a function of $u_* L/\nu$, which is a dimensionless variable proposed by Toba and Kunishi (1970) and Toba (1972, 1973) as the variable representing the overall degree of the breaking of wind waves, where u_* is the friction velocity of air, L the significant wave length, and ν the kinematic viscosity of air, the relation between θ_0 and $u_* L/\nu$ is not clearly found. However, the relation between θ observed at 6-m level and $u_* L/\nu$ is clearly recognized in the salt-mass class of $\log m \geqq 2.75$. This seems to suggest that very near the sea surface, $z = z_0$ is not appropriate as the production surface of sea-salt particles. The theoretical vertical gradient of θ is extremely large very near the sea surface ($z = 0$) and the weaker the wind speed, the more extremely large value of θ_0 appears. Consequently, when there is no wind, or there is only a weak breeze, if sea-salt particles produced before the observation are collected, the value of θ_0 becomes extermely large.

Then, it is necessary to consider an appropreate reference level of the production of sea-salt

particles. When there is some wind, the sea surface is not a plain surface. Since sea-salt particles are produced on the complicated rough surface, it may not be pertinent to adopt the surface $z = z_0$, which is veay near to the mean sea surface, $z = 0$, as the surface of the production of sea-salt particles. Although the relation between the production of sea-salt particles and wind waves are complicated, as the approximate representation, it is assumed that sea-salt particles produced at the part of wave surface above the mean sea surface ($z = 0$) are diffused in the lowest atmospheric layer above the sea surface. On this assumption, the surface, $z = z_1$ is newly introduced as the appropreate reference level of the production of sea-salt particles, as shown in Fig. 30.

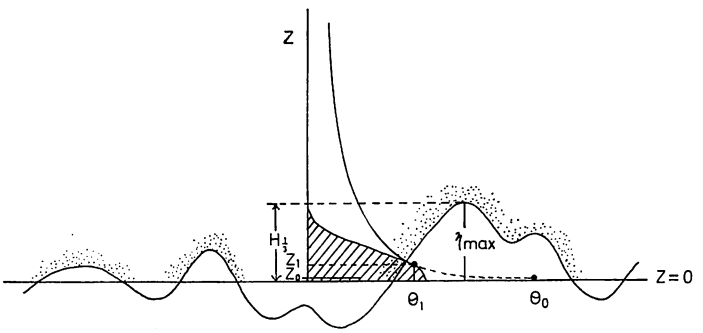

Fig. 30. Schematic representation of the present model near the sea surface.

This surface is decided from the statistical consideration, namely, the probability density distribution of the water level, η, in rough seas is generally expressed by the Gaussian distribution (Cox and Munk, 1954, Kinsman, 1960). The center in a half part of the Gaussian distribution of η, determines the surface, z_1, in the condition of waves under consideration. According to the Gaussian law of error, the distribution of probability density of η is expressed by

$$\phi(\eta) = \frac{1}{\sigma\sqrt{2\pi}} e^{\frac{-\eta^2}{2\sigma^2}} \tag{4.3}$$

where σ is the standard deviation. The $\phi(\eta)$ becomes nearly zero when $\frac{\eta}{\sigma} = 3$, and the point $\frac{\eta}{\sigma} = 3$ is denoted by η_{max}. Then, the distribution of probability density of the number concentration of sea-salt particles at the actual sea water surface is expressed by

$$\theta(z) = \theta_{z=0} e^{-\frac{9}{2}\left(\frac{z}{\eta_{max}}\right)^2} \tag{4.4}$$

The area of a half part of the Gaussian distribution is divided equally at $\frac{\eta}{\sigma} = 0.6745$. Consequently, if the point of $\frac{\eta}{\sigma} = 0.6745$ is expressed by z_1, the surface, z_1, for each observation of sea-salt partielcs is obtained from η_{max}. Namely,

$$z_1 = 0.6745\eta_{max}/3 \tag{4.5}$$

It is generally known that the maximum of water level, η_{max}, is nearly equal to the significant wave height, $H_{\frac{1}{3}}$ (Longuet-Higgins, 1952, Wiegel, 1949). By the use of the observed significant

wave period $T_{\frac{1}{3}}$ for each observation (the subscript of $\frac{1}{3}$ for $H_{\frac{1}{3}}$ and $T_{\frac{1}{3}}$ will be omitted hereafter), the values of H may be obtained using the three-second power law for wind waves by Toba (1972), as expressed by

$$H^* = 0.062\, T^{*\frac{3}{2}} \tag{4.6}$$

where $H^* = gH/u_*^2$, $T^* = gT/u_*$. The value of u_*, the friction velocity, is estimated approximately from U_{10} by the use of the relation $u_* = \gamma_{10}\, U_{10}$, together with the empirical formula by Deacon and Webb (1962), $\gamma_{10}^2 = (1.00+0.07U_{10})\times 10^{-3}$. By obtaining the value of H $(= \eta_{\max})$, the center, z_1, of the Gaussian distribution is easily estimated by equation (4.5). This surface is taken as the reference level of the production of sea-salt particles, and is called the z_1-surface.

The value of θ at the z_1-surface is expressed by θ_1, i. e., $\theta\,(z_1) = \theta_1$. The values of θ_1 for each class of salt-mass at the z_1-surface in each observation are obtained from θ-values at the height of 6 m, by the extrapolation according to the vertical distribution of sea-salt particles, in the condition of RH_{10} (eff.) = 95%. The salt-mass distributions of θ_1 for each wind force are shown in Fig. 31, and the mean distributions for various wind forces are shown in Fig. 32. The features of the salt-mass distribution of θ_1 for the salt-mass class of $\log m \leqq 2.5$ for wind forces 3, 4 and 5 are close to straight lines and parallel to each other, and the Junge distribution, stated in the salt-mass distribution of θ, still holds at the z_1-surface. It is seen in Fig. 32 that the salt-mass distributions of θ_1 for $\log m \leqq 1.75$ for wind force 2 and $\log m \leqq 2.25$ for wind force 6 do not show a straight line as those for wind force 3, 4 and 5. The reason is attributed to the distribution of θ. The value of θ_1 for $\log m > 3$ does not largely change with increasing $\log m$, from the data obtained up to $\log m = 5$ in wind force 7, the pattern having a small

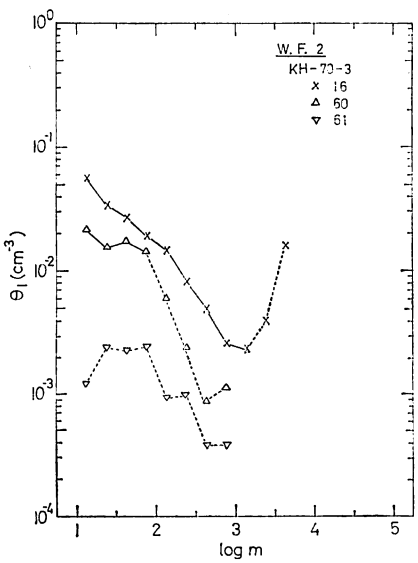

Fig. 31 (a)

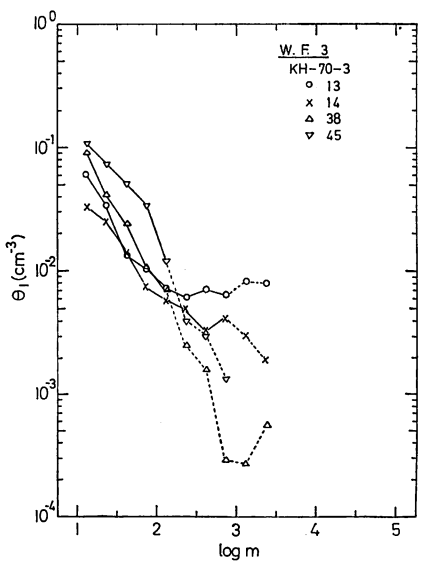

Fig. 31 (b)

Fig. 31. Values of θ_1 reduced from Fig. 24 by the modified equiliblium vertical distribution for $RH_{10} = 95$ %, (a) in wind force 2. (b) wind force 3, (c) wind force 4, (d) wind force 5, (e) wind force 6 and (f) wind force 7.

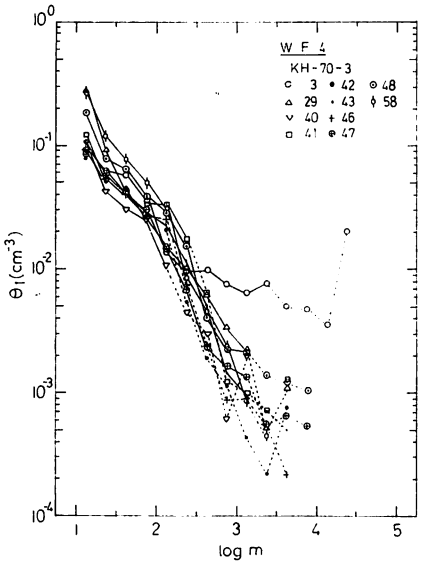

Fig. 31 (c)

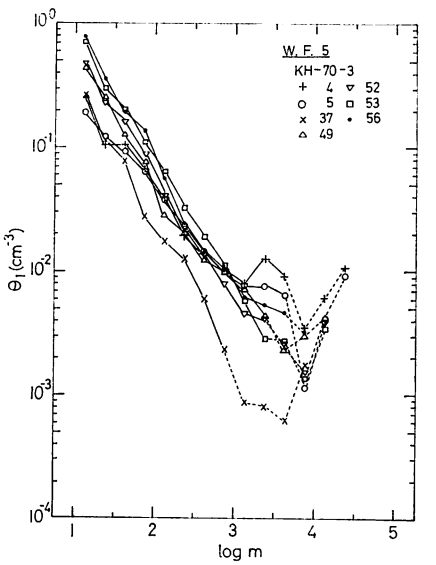

Fig. 31 (d)

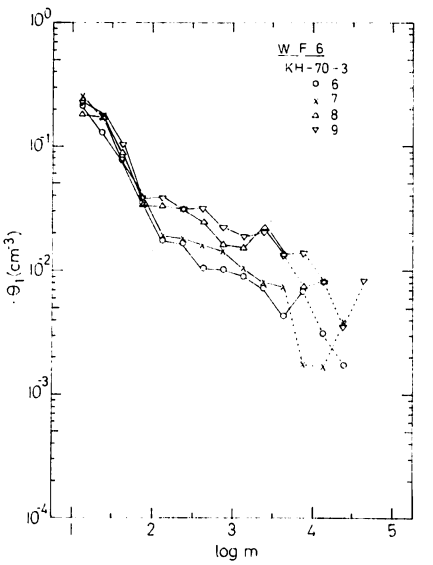

Fig. 31 (e)

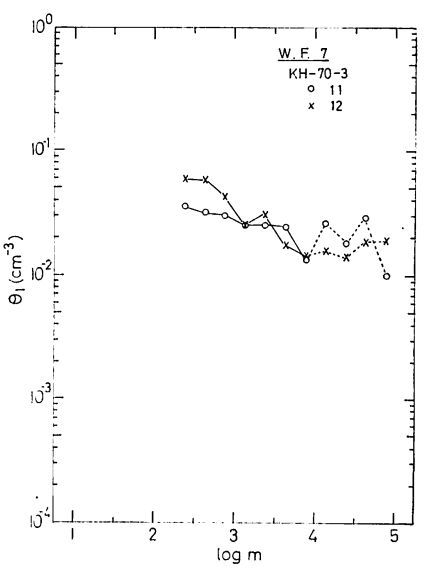

Fig. 31 (f)

trough near $\log m = 4$ is estimated.

Now, the representative curve of salt-mass distribution of θ_1 for the range of $\log m = 1 \sim 5$ can be determined. This has been obtained by connecting the left straight part for wind force 5 with the smoothed curve of salt-mass distribution for wind force 7. The smoothing has been performed by the method of running mean over three points. They are shown with dashed lines in Fig. 32. The representative curves are entered so that curves for wind force 4 and 5 fit the points as close as possible, because the data for wind force 4 and 5 contains a large original numbers of observation. The intervals among the representative curves for various wind forces are

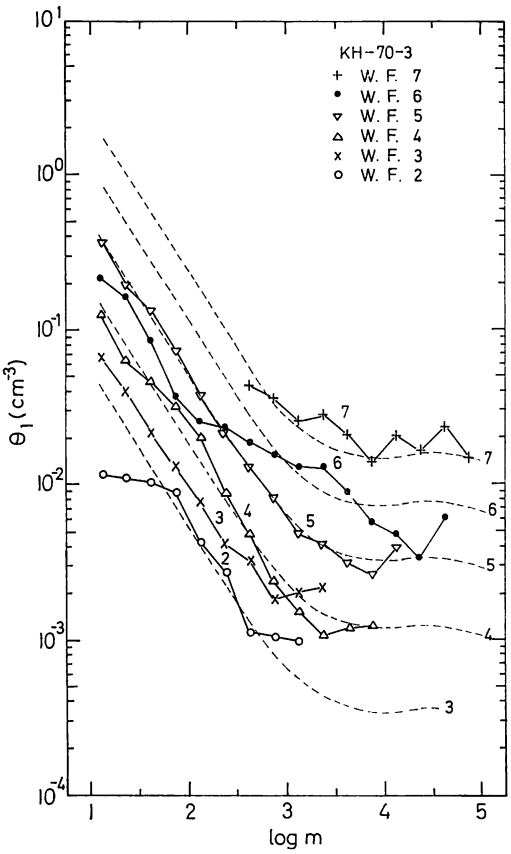

Fig. 32. Mean salt-mass distribution of θ_1 for each wind force for KH-70-3 data (from Fig. 31).

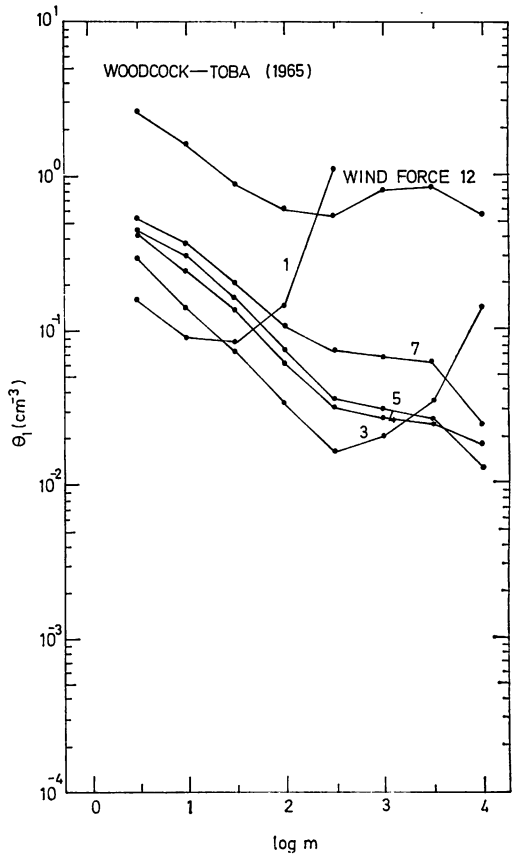

Fig. 33. Salt-mass distribution of θ_1 for each wind force for Woodcock-Toba data. Values are entered for ranges of $\log m = 0.5$

decided as described below.

The production rate of sea-salt particles depends on the dimensionless variable, u_*L/ν, as will be described in the next section, 4. 2. The value of u_*L/ν corresponding to each wind force is obtained from the equation (Toba, 1972) expressed below,

$$\frac{u_*L}{\nu} = \frac{\gamma^3 T^{*2}}{2\pi g\nu} U_{10}^3 \tag{4.7}$$

using the median wind speed for each wind force, where the value of γ of 0. 040, and value of T^* of 94 are used. The value of T^* of 94 is obtained from the equation,

$$T^* = 2\pi\beta/\gamma$$

by assuming the wave age $\beta = C/U = 0.6$, which corresponds to the case where wind speed is ten and several m sec^{-1} blowing for several hours. The value of kinematic viscosity of air, ν of 0. 157 cm^2 sec^{-1}, for the temperature of 25°C, is also used.

Comparing the mean salt-mass distribution of θ_1 with the representative one, both the curves

are not in agreement in wind force 7, and the values of the representative curve are smaller than those of the observed mean values in each class of salt mass. This may be attributed to small number of observations in wind force 7. In wind conditions weaker than wind force 3, the values of θ_1 in the mean salt-mass distribution are higher than that in the representative curves. It is considered that the relatively high values of θ_1 in wind forces 2 and 3 are attributed to the sea-salt particles suspended in the air before the sampling. Although the agreement in the number concentrations of sea-salt particles between the mean salt-mass distribution of θ_1 and that of the representative curve is not exact for some wind forces, the character of the salt-mass distribution of θ_1 for various wind forces may be regarded as always same, and the absolute value changes according to the change of the states of the wind and wind waves.

From the data of the salt-mass distribution of θ by Woodcock-Toba, that of θ_1 was obtained as shown in Fig 33. The z_1-surfaces for various wind forces were calculated from the significant wave height, H, corresponding to the median wind speed of each wind force, by the use of equation (4. 6). Namely, since,

$$H^* = gH/u_*^2 = gH/\gamma^2 U_{10}^2$$

equation (4. 6) is expressed by

$$H = 0.062 T^{*\frac{3}{2}} \gamma^2 U_{10}^2/g \qquad (4.8)$$

The value of T^* of 94 adopting in equation (4. 7) was also used. As shown in Fig. 33, the salt-mass distribution of θ_1 of $\log m \leqq 2.5$ has a curve close to a straight line, but the situation of the distribution is not expressed by the Junge distribution. The values of θ_1 for the salt-mass class of $\log m \geqq 2.5$ are nearly the same values for the wind force stronger than 4, though the value of $\log m = 4$ becomes relatively low. The values of θ_1 for wind forces 1 and 3 increased with salt mass for larger values of $\log m$. It is seen in the figure that there is a similar tendency which was found in the salt-mass distribution of θ_0. In this case, the tendency also may be caused by the coalescence of sea-salt particles as already discussed by Toba (1965 a).

4. 2. A factor governing the production of sea-salt particles

Concerning the relation between sea-salt particles and wind speed, Toba (1961) obtained the dependence of the rate of droplet production on wind speed (m sec^{-1} at 10-m level) expressed by approximately exp (0. 40 U) in the range of the wind speed between 15 m sec^{-1} and 23 m sec^{-1}, using the results of wind flume experiments. Chaen (1971) also obtained a similar relation on the basis of the results of the observations in the Indian Ocean. However, it is more proper to consider the relation between the number concentration of sea-salt particles and the strength of turbulence of the wave field that is related with both of wind and wind waves, because the production of sea-salt particles is related to the air entrainment in wind waves and the bursting of air bubbles.

Takahashi (1958) discussed relations between the friction velocity, u_*, and wind waves from his data of winds and wind waves observed in Kagoshima Bay, and estimated an empirical value of the critical friction velocity of about 17 cm sec^{-1} for generation of whitecaps. This result was obtained from the data observed in a relatively small sea area. Concerning the value of the

strength of turbulence of the wave field, Toba and Kunishi (1970) introduced a kind of Reynolds number u_*H/ν or u_*L/ν, as representing the strength of turbulence of wind wave field, and showed that the breaking of wind waves commences as u_*H/ν reaches 1×10^3, using the results of wind flume experiments. More recently, Toba (1972, 1973) has proposed his third concept that the overall degree of the breaking of wind waves is expressed by u_*L/ν.

In the present article, the demensionless variable u_*L/ν is adopted, as the variable representing the strength of turbulence of the wind wave field. The relation between the number concentration, θ, or its value at the z_1-surface, θ_1, and u_*L/ν are discussed. The dimensionless variable u_*L/ν at the time of observation of sea-salt particles may be obtained from the data of the significant wave period, T, and the wind speed at 10-m level, U_{10} according to the following manners. The value of u_* has been estimated from U_{10} by the relation, $u_* = \gamma_{10}U_{10}$, togather with the formula by Deacon and Webb (1962), L has been obtained by $L = gT^2/2\pi$, where g is the acceleration of gravity.

The relation between the number concentration of sea-salt particles at 6-m level, θ, for the ranges of $\log m = 0.5$, and u_*L/ν is shown in Fig. 34. It is seen in the figures that θ increases linearly with u_*L/ν on the $\log\theta - \log u_*L/\nu$ diagram, and fine relations are found for the salt-mass classes of $\log m \geqq 2.25 \sim 2.75$. The gradient of the distribution of θ on the logarithmic diagram increases clearly with the increasing class of salt mass. From the figures, the following empirical formulas are proposed concerning the value of θ at a height of 6 m :

$$
\begin{aligned}
&\log\theta = 0.7\log(u_*L/\nu) - 4.4, && (\log m < 1.25)\\
&\log\theta = 0.7\log(u_*L/\nu) - 4.5, && (1.25 < \log m < 1.75)\\
&\log\theta = 0.7\log(u_*L/\nu) - 5.1, && (1.75 < \log m < 2.25)\\
&\log\theta = 0.8\log(u_*L/\nu) - 6.5, && (2.75 < \log m < 2.75) \qquad (4.9)\\
&\log\theta = 1.4\log(u_*L/\nu) - 10, \quad \text{for } u_*L/\nu \geqq 5\times10^4 && (2.75 < \log m < 3.25)\\
&\log\theta = 1.6\log(u_*L/\nu) - 12, \quad \text{for } u_*L/\nu \geqq 5\times10^4 && (3.25 < \log m < 3.75)\\
&\log\theta = 1.9\log(u_*L/\nu) - 15, \quad \text{for } u_*L/\nu \geqq 5\times10^4 && (3.75 < \log m < 4.25)
\end{aligned}
$$

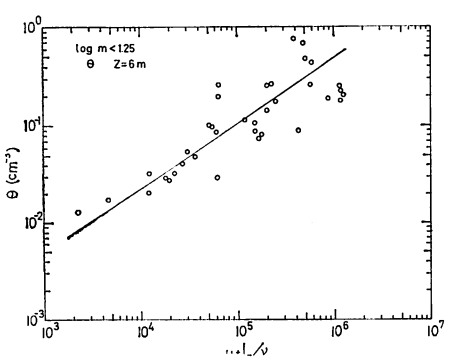

Fig. 34 (a)

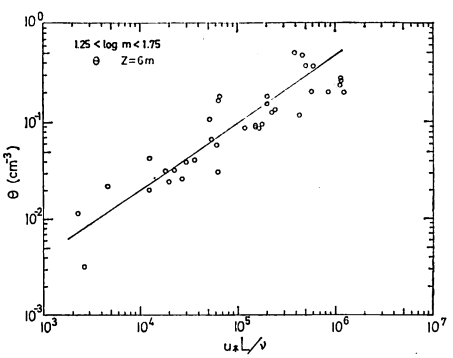

Fig. 34 (b)

Fig. 34. Values of the number concentration of sea-salt particles, θ, at 6-m level for each salt-mass class, plotted against u_*L/ν, (a) salt-mass class of $\log m < 1.25$, (b) $1.25 < \log m < 1.75$, (c) $1.75 < \log m < 2.25$, (d) $2.25 < \log m < 2.75$, (e) $2.75 < \log m < 3.25$, (f) $3.25 < \log m < 3.75$ and (g) $3.75 < \log m < 4.25$. The straight lines indicate the formulas (4.9).

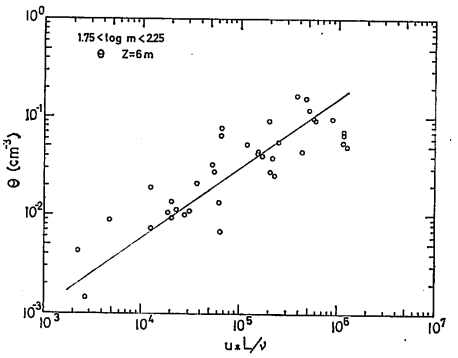

Fig. 34 (c)

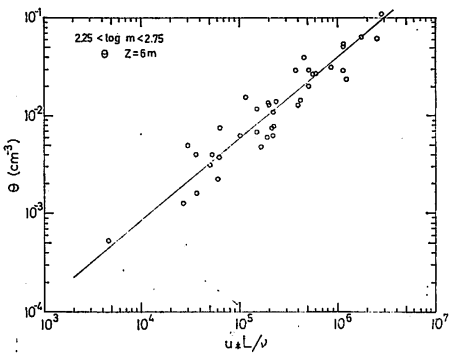

Fig. 34 (d)

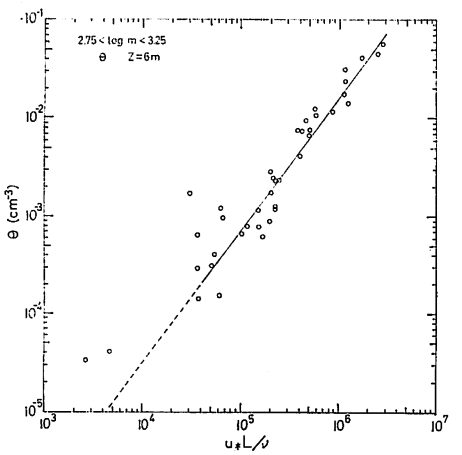

Fig. 34 (e)

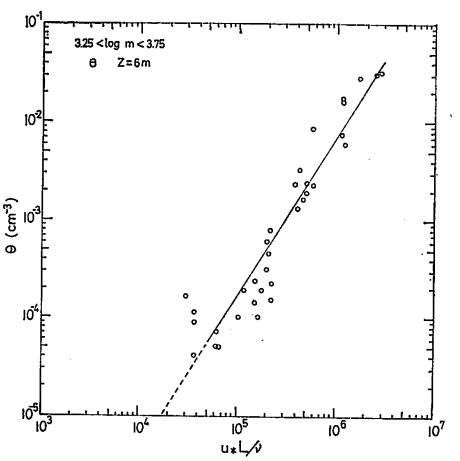

Fig. 34 (f)

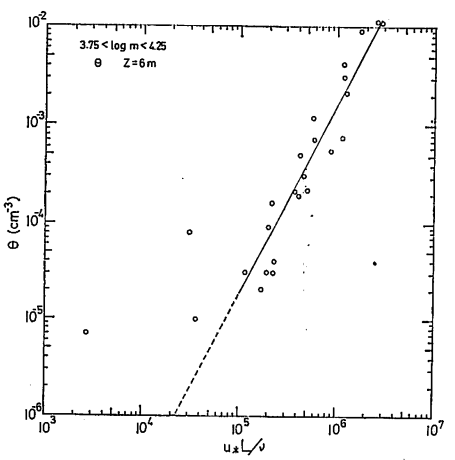

Fig. 34 (g)

The straight lines entered in Fig. 34 show these formulas. The formula may be applied for larger values of u_*L/ν than 5×10^4 in the salt-mass class of $\log m \geqq 2.75$. The factor of proportionality gradually increases with the salt-mass. This fact shows that sea-salt particles of $\log m \geqq 2.75$ well represent a rather local condition of the wave breaking, whereas particles of $\log m \leqq 2.25$ seem to represent conditions more than a few hours before the sampling. The above-

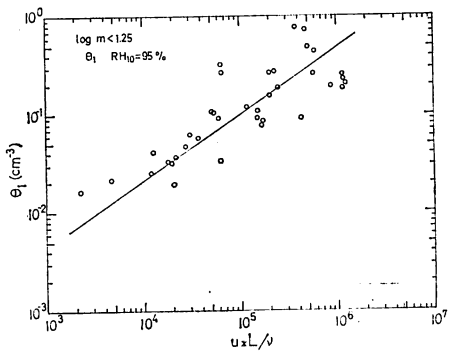

Fig. 35 (a)

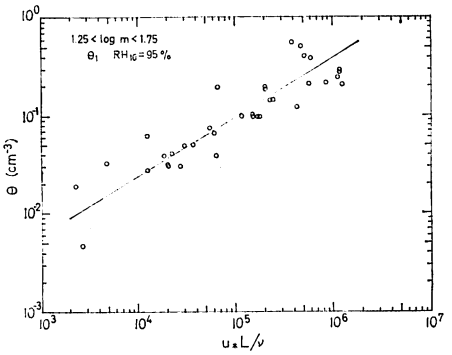

Fig. 35 (b)

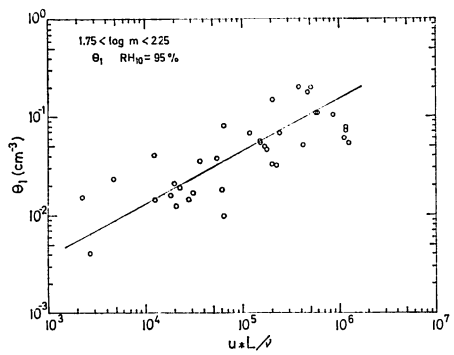

Fig. 35 (c)

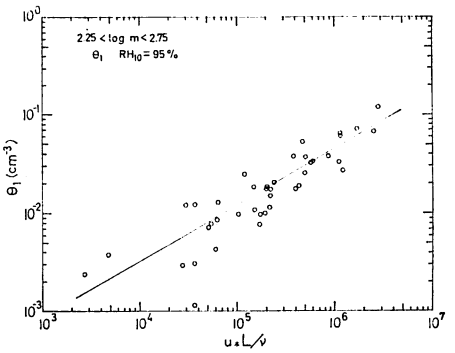

Fig. 35 (d)

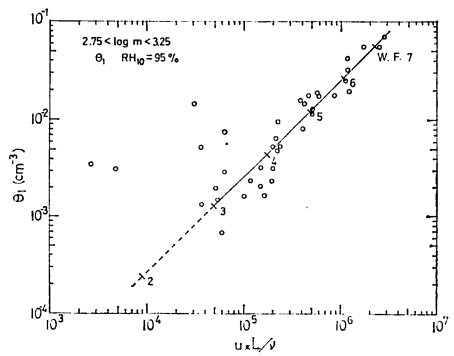

Fig. 35 (e)

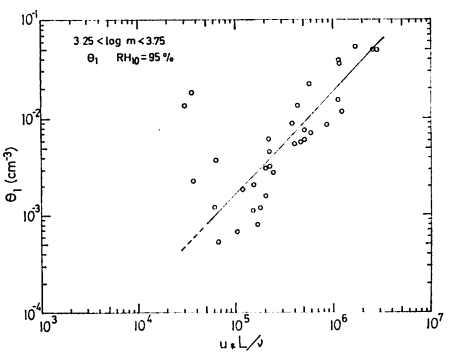

Fig. 35 (f)

Fig. 35. Values of the number concentration of sea-salt particles, θ_1, at the z_1-surface, for each salt-mass class, plotted against u_*L/ν(a) salt-mass class of $\log m < 1.25$, (b) $1.25 < \log m < 1.75$, (c) $1.75 < \log m < 2.25$, (d) $2.25 < \log m < 2.75$, (e) $2.75 < \log m < 3.25$, (f) $3.25 < \log m < 3.75$ and (g) $3.75 < \log m < 4.25$. The straight lines indicate the formulas (4. 10).

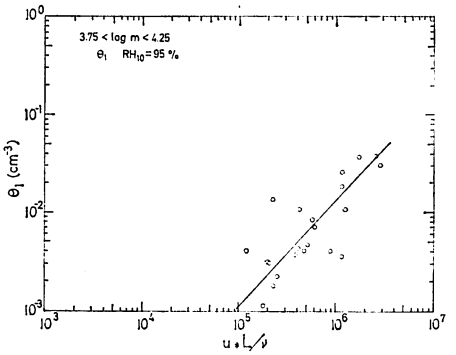

Fig. 35 (g)

mentioned results indicate that the number concentration of sea-salt particles in the lowest atmospheric layer above the sea surface may be used as an indicator representing the supply of turbulent energy into the upper ocean by the breaking of wind waves.

In Fig. 35 are shown the relation between the number concentration at the z_1-surface, θ_1, and u_*L/ν. The relation is almost same as that between θ and u_*L/ν for the salt-mass class of $\log m \leqq 2.25$, but the value of θ_1 is proportional to u_*L/ν for $u_*L/\nu \geqq 5\times10^4$ in the salt-mass class of $\log m \geqq 2.75$. These empirical formulas are as follows :

$$
\begin{aligned}
&\log\theta_1 = 0.7(u_*L/\nu)-4.4, && (\log m < 1.25)\\
&\log\theta_1 = 0.6(u_*L/\nu)-4.1, && (1.25 < \log m < 1.75)\\
&\log\theta_1 = 0.5(u_*L/\nu)-4.0, && (1.75 < \log m < 2.25)\\
&\log\theta_1 = 0.6(u_*L/\nu)-4.8, && (2.25 < \log m < 2.75)\\
&\log\theta_1 = 1.0(u_*L/\nu)-7.6, \quad \text{for } u_*L/\nu \geqq 5\times10^4 && (2.75 < \log m < 3.25)\\
&\log\theta_1 = 1.1(u_*L/\nu)-8.1, \quad \text{for } u_*L/\nu \geqq 5\times10^4 && (3.25 < \log m < 3.75)\\
&\log\theta_1 = 1.1(u_*L/\nu)-8.4, \quad \text{for } u_*L/\nu \geqq 5\times10^4 && (3.75 < \log m < 4.25)
\end{aligned}
\qquad (4.10)
$$

The straight lines entered in Fig. 35 show the formulas. The value of u_*L/ν for each wind force was calculated from equation (4.7), using the median wind speed of each wind force, and it is entered on the straight line representing the formula for the salt-mass class of $\log m = 2.75\sim 3.25$ (Fig. 35 e). The starting value of u_*L/ν from which θ_1 is propotional to u_*L/ν in the salt-mass class of $\log m \geqq 2.75$ nearly corresponds to wind force 3. This result demonstrates that the production of sea-salt particles, i. e., the breaking of wind waves begins to take place at the value of u_*L/ν of 5×10^4, which corresponds to wind force 3 in the sea. The factors of proportionality of the formulas for the salt-mass class of $\log m \leqq 2.75$ are small compared with those for $\log m \geqq 2.75$. This seems to be caused by the collection of the sea-salt particles which were suspended in the air before the sampling.

On the other hand, the relation between the value of θ_0, the number concentration of sea-salt particles at $z = z_0$ very near the sea surface, and u_*L/ν is not fine, i. e., the points are more scattered, as shown in Fig. 36. This seems to support the idea that the value of θ_0 is unreasonable as the sea surface value, as described in the previous section.

As the other evidence representing the relation between the number concentration of sea-salt particles and the overall degree of the breaking of wind waves, θ-values at 6-m level are

plotted against P-values (%), the portion of the breaking area to the whole area of sea surface in a visual field of a camera (Toba and Chaen, 1973). It is seen that θ of $\log m \geqq 2.75$ is proportional to the P-value, as shown in Fig. 37. Toba and Chaen (1973) showed the commencement of the breaking of wind waves is located at 2×10^4 in u_*L/ν, from the relation between P-values (%) and u_*L/ν.

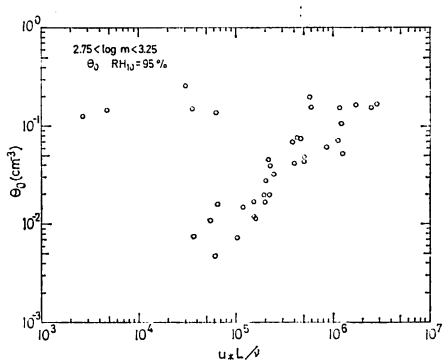

Fig. 36(a)

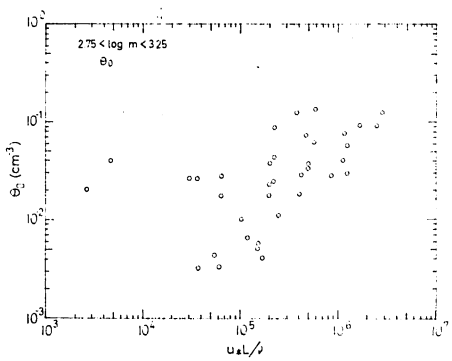

Fig. 36(b)

Fig. 36. Values of the number concentration of sea-salt particles, θ_0, at $z = z_0$, for the salt-mass class of $\log m = 2.75\sim3.25$, plotted against u_*L/ν, (a) at the condition of $RH_{10} = 95\%$ and (b) observed RH_{10}.

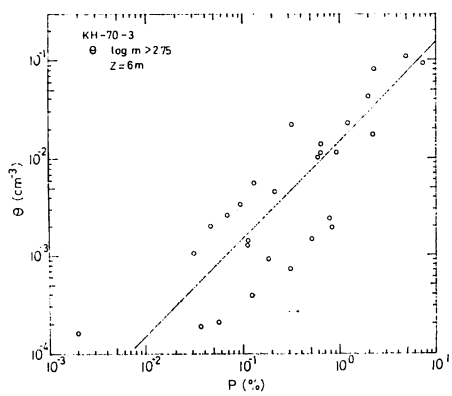

Fig. 37. Values of the number concentration of sea-salt particles, θ, for $\log m \geqq 2.75$ at 6-m level, plotted against P-values, the portion of the breaking area to the whole area of sea surface in a visual field of a camera (Toba and Chaen, 1973). The straight line indicates the formula, $\log \theta = 1.0 \log (P) - 1.8$.

4.3. Production rate of sea-salt particles

From equation (3. 1), the production rate, F_1 ($cm^{-2}sec^{-1}$), at the z_1-surface, or the actual sea surface, or the upward flux of the particles, which balances with the downward flux, is understood as,

$$F_1 = w_s\theta_1 \tag{4. 11}$$

where w_s represents the terminal velocity of sea-water droplet. Fig. 38 shows the estimated values of F_1, calculated from the values in Fig. 31 by equation (4. 11), and the mean salt-mass distributions of F_1 for various wind forces are shown in Fig 39. The dashed lines are the representative curves of F_1 in the range of $\log m = 1\sim5$, also calculated from those in Fig. 32. The

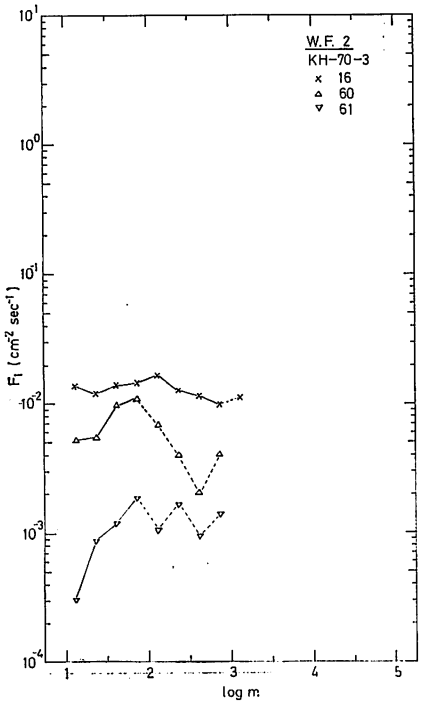

Fig. 38 (a)

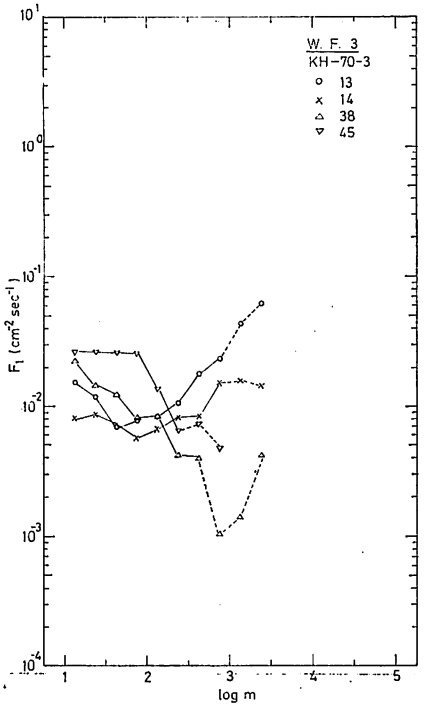

Fig. 38 (b)

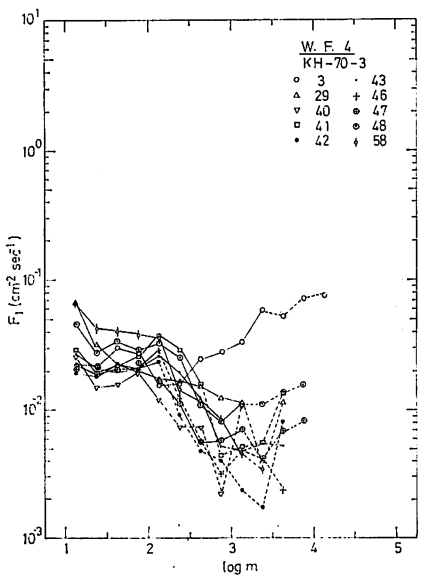

Fig. 38 (c)

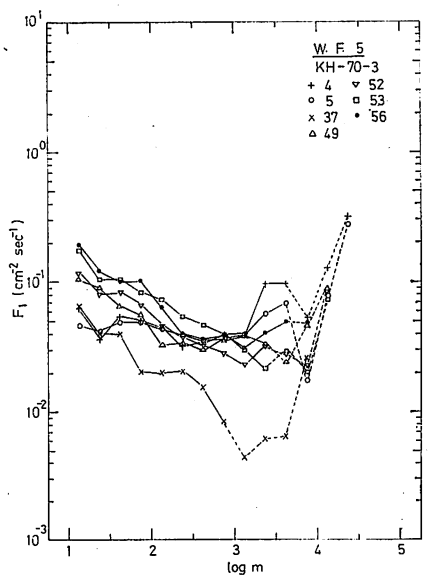

Fig. 38 (d)

Fig. 38. Values of F_1, calculated from the θ_1-values in Fig. 31 by $F_1 = w_s \theta_1$, (a) in wind force 2, (b) wind force 3, (c) wind force 4, (d) wind force 5, (e) wind force 6 and (f) wind force 7.

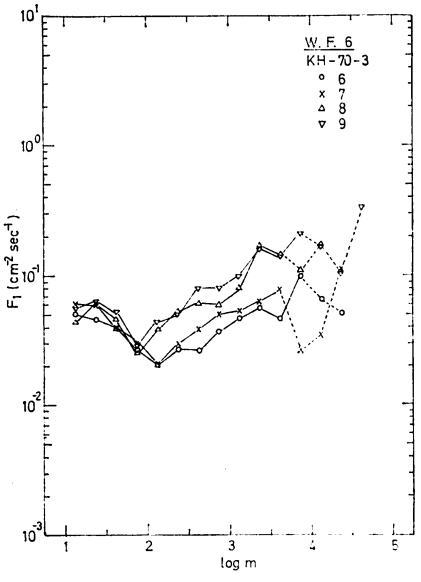

Fig. 38 (e)

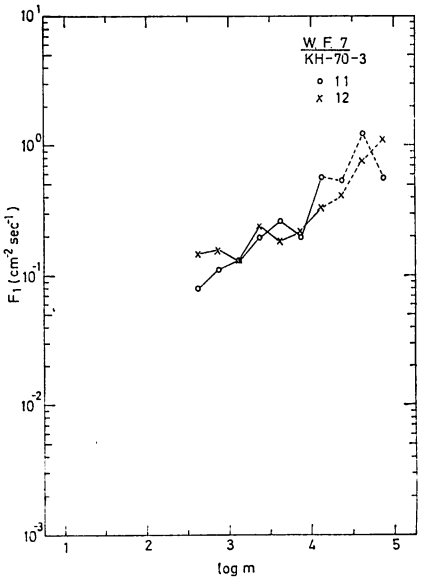

Fig. 38 (f)

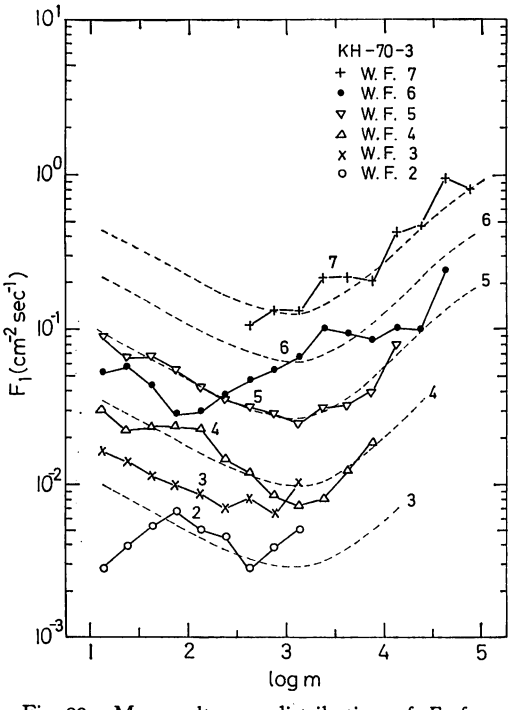

Fig. 39. Mean salt-mass distribution of F_1 for each wind force for KH-70-3 data (from Fig. 38). The dashed lines indicate the representative curves of F_1, calculated from those in Fig. 32 by $F_1 = w_s\theta_1$

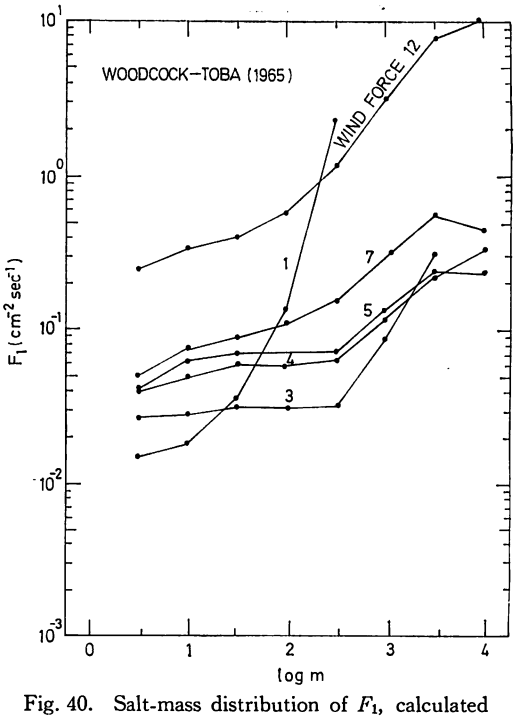

Fig. 40. Salt-mass distribution of F_1, calculated from the θ_1-values in Fig. 33 (Woodcock-Toba data) by $F_1 = w_s\theta_1$.

intervals of those curves for various wind forces are determined from the relation between F_1 and u_*L/ν as described in relation to the salt-mass distribution of θ_1, and the curves are entered in Fig. 39 in such a manner that the curves for wind forces 4 and 5 fit the mean salt-mass distributions for wind forces 4 and 5 as close as possible. As clearly seen in Fig. 39, the salt-mass distribution of F_1 has a minimum value at $\log m = 3$, and from this point, it increases with the decreasing and the increasing salt mass. Comparing the mean salt-mass distributions for various wind forces with the representative curves, it is reasonable to conclude that the character of the curves is always same and independent of the wind speed, though there are some disagreements in the values of F_1 as mentioned in the distribution of θ_1.

As a comparison, the salt-mass distributions of F_1 for various wind forces have also been estimated from Fig. 33 by $F_1 = w_s\theta_1$ which was θ_1 values obtained from Woodcock-Toba values of θ. The values are shown in Fig. 40. The values of F_1 for the salt-mass class of $\log m = 0.5$ are low, and gradually increase with the salt mass up to $\log m = 2.5$, and then, the values of F_1 sharply increase with the salt mass up to $\log m = 3.5$. Although there are some differences between the salt-mass distribution of F_1 in the present article and that estimated from Woodcock-

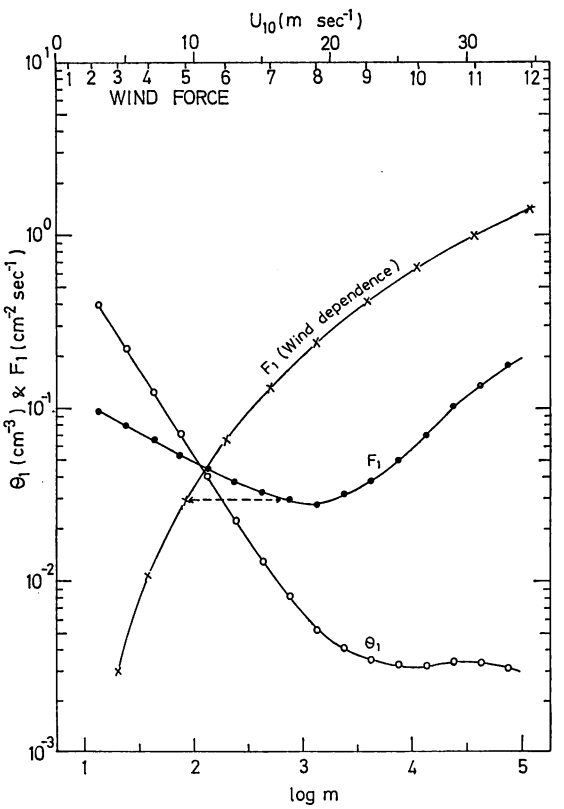

Fig. 41. Representative curves for the production rate, F_1, the number concentration, θ_1, at the z_1-surface and wind dependence of F_1. Values of F_1 and θ_1 are entered for wind force 5, and the values of wind dependence of F_1 are entered for $\log m = 2.75 \sim 3.0$.

Table 4. Number concentration of sea-salt particles at the z_1-surface, θ_1, the terminal velocity of sea-water droplets, w_s, and the production rate of sea-salt particles, F_1, for $u_*L/\nu = 4.9 \times 10^5$. The values of θ_1 and F_1 for other values of u_*L/ν may be obtained from the tabulated values, by the use of the relation that both θ_1 and F_1 are proportional to u_*L/ν. If the sea surface conditions or waves are regarded as a function only of wind speed, the value of u_*L/ν corresponds to wind force 5, and values for other wind forces may be obtained by the use of the multiplication factor in the table for each wind force.

Range of mass of salt	$\log m =$ 1	1.5	2	2.5	3	3.5	4	4.5	5
θ_1(10^{-2}, cm^{-3})	39.2	22.2	12.4	7.02	3.92	2.23	1.30	0.815	0.522	0.410	0.348	0.325	0.325	0.340	0.330	0.310
w_s (cm sec^{-1})	0.244	0.355	0.521	0.760	1.15	1.66	2.49	3.62	5.22	7.70	10.6	15.2	21.2	29.5	41.3	58.0
F_1(10^{-2}, cm^{-2} sec^{-1})	9.56	7.88	6.46	5.34	4.51	3.70	3.24	2.95	2.72	3.16	3.69	4.94	6.89	10.0	13.6	18.0

Wind force	3	4	5	6	7	8	9	10	11	12
Multiplication factor to be applied to the above values of θ_1 and F_1	0.105	0.367	1	2.24	4.51	8.19	14.1	22.4	34.2	49.8

Toba data, the order of magnitude is in agreement. A significant point of the difference between the two is that there is no minimum at near $\log m = 3$ in the latter. This is caused by the small value of θ in the salt-mass class of $\log m \leqq 3$.

As there is a clear relation between θ_1 and u_*L/ν, there is also the definite relation between F_1 and u_*L/ν, since F_1 and θ_1 are related by $F_1 = w_s\theta_1$. The F_1 for the classes of salt mass of $\log m \geqq 2.75$ which represent the local conditions of the particle production, is proportional to u_*L/ν. This fact fully supports Toba's conception (1972, 1973) that the overall degree of the breaking of wind waves is proportional to the dimensionless variable u_*L/ν.

As discussed so far, the values of θ_1 and F_1 depend on the states of wind and wind waves, specifically speaking, these are proportional to u_*L/ν. It is practically convenient, however, if the salt-mass distributions of θ_1 and F_1 are presented as the function of wind speed alone, as an approximation, instead of as the function of u_*L/ν, which include the sea state as well as the wind speed. These relations are summarized in Fig. 41. In the figure, the representative salt-mass distributions of θ_1 and F_1 for wind force 5 are presented, and as to the wind dependence of F_1, the curve for $\log m = 2.75 \sim 3.0$ is presented as the function of wind speed alone as an approximation, instead of as the function of u_*L/ν, from the fact that the F_1 is proportional to the dimensionless variable u_*L/ν. By the use of Fig. 41, the salt-mass distribution of θ_1 and F_1 for various wind forces can be predicted by the parallel translation of the curves for wind force 5, on the basis of the intervals among wind forces on the curve of wind dependence. The values of θ_1 and F_1 for each class of $\log m$ for wind force 5, and w_s for each class of $\log m$ are tabulated in Table 4, together with multiplication factors for various wind forces.

5. Summary and Conclusion

Systematic observations of sea-salt particles, wind and wind waves were carried out on board ships at sea, in order to determine the amount of sea-salt particles in the lowest atmospheric layer above the sea surface and their production rates on the sea surface empirically.

Using two kinds of samplers, a hand-operated impactor and a rod sampler, materials in a

wide range of salt mass from 10^{-11} gm to 10^{-7} gm has been obtained. The efficiency of impaction of the rod sampler is estimated to be about 80% or more for sea-salt particles of $\log m \geqq 2.5$.

The mean vertical distribution of the number concentration of sea-salt particles, θ, in the lowest atmospheric layer above the sea surface is very close to a stright line on the logarithmic diagram of $\log z - \log \theta$, though individual distribution is variable. The mean vertical gradient of θ is approximately expressed by a modified equilibrium theory introducing the effective relative humidity of 95 % at 10-m level. This is concluded from the comparision between the observed gradient and theoretical one calculated by Toba's theory, and is confirmed also from simultaneous two kinds observation of the reagent film and the MgO surface.

The feature of the mean salt-mass distribution of θ for each wind force is close to a straight-line segment for the salt-mass class of $\log m \leqq 2.25$, and they are parallel to each other. The distribution is approximately expressed by the Junge's form concerning aerosols in the atmosphere.

The reference level of the production of sea-salt particles, the z_1-surface, is newly introduced from the statistical consideration of wind waves. The number concentration of sea-salt particles at the z_1-surface, θ_1 is determined by extrapolating the observed vertical distribution of θ. The feature of the salt-mass distribution of θ_1 for each wind force is close to a straight-line segment for the salt-mass class of $\log m \leqq 2.5$, and it is expressed by the Junge's form. The value of θ_1 in the distribution does not largely change with increasing $\log m$. Synthesizing the obtained mean salt-mass distribution of θ_1, the representative curve of the mean salt-mass distribution of θ_1, has been determined. The character of the distribution curve may be regarded as always same, and only the absolute value changes according to the change of states of the wind and wind waves.

The relationships are examined between the number concentration of sea-salt particles, θ, the value at the z_1-surface, θ_1, and the demensionless variable u_*L/ν, which represents the overall degree of the breaking of wind waves. The θ increases linearly with u_*L/ν on the log θ–log u_*L/ν diagram, and fine relations are found for the classes of salt mass of $\log m \geqq 2.25 \sim 2.75$. This result indicates that the number concentration of sea-salt particles may be used as an indicator representing the overall degree of the breaking of wind waves. The values of θ_1 for the salt-mass class of $\log m \geqq 2.75$ increase in proportion to u_*L/ν. On the other hand, u_*L/ν has not a clear relation with θ_0, the θ-value at a surface of z_0, which was used by Toba (1965 a) as the sea-surface value, where z_0 is roughness parameter.

The production rate of sea-salt particles, F_1 ($\mathrm{cm^{-2}\ sec^{-1}}$), or upward flux of the particles, which balanecs with downward flux at the sea surface, were obtained from the values of θ_1 at the z_1-surface, by $F_1 = w_s\theta_1$. The salt-mass distribution of F_1 has the minimum value at $\log m = 3$ in the $\log F_1 - \log m$ diagram. The character of the salt-mass distribution curve of F_1 may also be regarded as always same with changing value of u_*L/ν. The values of F_1 also may be regarded as proportional to u_*L/ν, since θ_1 is proportional to u_*L/ν. This supports the treatment by Toba (1972, 1973) that the overall degree of the breaking of wind waves is proportional to u_*L/ν.

As conclusion, the values of θ_1 and F_1 for each class of salt mass are presented as a function of u_*L/ν; and also, as an approximation, they may be tentatively expressed as a function of wind

speed alone, namely, by assuming representative state of sea surface as a function of wind speed.

The results obtained in the present study are conclusions concerning the production rate of sea-salt particles on the sea surface. They will become basic data for problems of the air-sea boundary processes, such as evaporation from the sea surface, energy supply to surface waves, turbulence and drift current in the surface layer, friction coefficient, as well as to scientific problems, such as cloud physics, estimate of the wind distribution over global oceans from a satellite, radiation problems of the atmosphere-ocean system, geochemistry, and prevention of salt damage.

Acknowledgments

The author wishes to express his sincere thanks to Prof. Tadao Takahashi of kagoshima University, Prof. Yoshiaki Toba of Tohoku University for their cordial guidance and encouragement throughout this study. Especially, Prof. Toba collaborated in the observation on board the R. V. Hakuhō Maru, and also provided the author with original data obtained at the Shirahama Oceanographic Tower Station by Toba et al. (1971). He thanks Prof. Shōitirō Hayami, Dean of the College of Marine Science and Technology, Tokai University for his encouragement. He also thanks Prof. Hideaki Kunishi of Kyoto University and Mr. Masaaki Tanaka, Disaster Prevention Research Institute, Kyoto University for their useful suggestions and encouragement. Concerning the observations, he thanks Capt. Soichi Ueda of the Kagoshima Maru, Kagoshima University and his crew, also Dr. Yoshimitsu Ogura, Chief Scientist of the GARP Cruise, Mr. Atsushi Takeda, Chief Scientist of the 2nd GARP Cruise, and the crews of the R. V. Hakuhō Maru, for their kind arrangements during the curise. He thanks Mr. Kuniaki Okuda, now at Geophysical Institute, Tohoku University, who collaborated in the observation of the 2nd GARP Cruise. He is deeply indebted to Miss Akiko Kamiaraiso for her assistance in the drawing.

References

Blanchard, D. C. (1963) : The electrification of the atmosphere by particles from bubbles in the sea. *Progress in Oceanography*, Pergamon Press, Oxford etc., Vol **1**., 71–202.

Blanchard, D. C, and A. H. Woodcock (1957) : Bubble formation and modification in the sea and its meteorological significance. *Tellus*, **9**, 145–158.

Chaen, M. (1971) : Observations of giant sea-salt particles in the sea-surface boundary layer. *Mem. Fac. Fish. Kagoshima Univ.*, **20** (1), 55–72.

Chaen, M. (1972) : Supplementary note on the previous papers, "Observations of the distribution of giant sea-salt particles in the sea-surface boundary layer" and "On the variation of the amount of giant sea-salt particles near the ground." *Mem. Fac. Fish. Kagoshima Univ.*, **21** (1), 125.

Cox, C. S. and W. H. Munk (1954) : Statistics of the sea surface derived from sun glitter. *Jour. Mar. Res.*, **13**, 198–227.

Deacon, E. L. and E. K. Webb (1962) : Interchange of properties between sea and air. Ch. 3. Small-scale interaction. in *The Sea*, edited by M. B. Hill, Interseience, New York, 43–87.

Duce, R. A., W. Stumm and J. M. Prospero (1972) : Working symposium on sea-air chemistry : Summary and Recommendations. *Jour. Geophys. Res.*, **77**, 5059–5061.

Farlow, N. H. (1954) : An improved halide ion-sensitive sampling surface for water aerosols. *Rev. Sci. Instr.*, **25**, 1109–1111.

Farlow, N. H. (1957) : Quantitative determination of chloride ion in 10^{-6}–to 10^{-12}-gram particles. *Anal.*

Chem. **29**, 883–885.

Farlow, N. H. (1958) : A method for measuring water content of airborne sea-salt particles. *Jour. Met.*, **15**, 228–230.

Fournier d'Albe, E. M. (1951) : Sur les embruns marins. *Bull. Inst. Océanogr.*, No. 995.

Hayami, S. and Y. Toba (1958) : Drop production by bursting of air bubbles on the sea surface (1), Experiments at still sea water surface. *Jour. Oceano. Soc. Japan*, **14**, 145–150.

Junge, C. E. (1953) : Die rolle der aerosole und der gasförmigen Beimengungen der Luft in spurenstoffhaushalt der troposphäre. *Tellus*, **5**, 1–26.

Junge, C. E. (1958) : Atmospheric chemistry, *Advances in Geophysics*, **4**, Academic Press, New York, 1–108.

Kientzler, C. F, A. B. Arons, D. C. Blanchard and A. C. Woodcock (1954) : Photographic investigation of the projection of droplets by bubbles bursting at a water surface. *Tellus*, **6**, 1–7

Kikuchi, K. and S. Yaura (1970) : Observations of giant sea-salt particles over the ocean from Tokyo to Showa station, Antarctica. *Jour. Meteor. Soc. Japan Ser* II, **48**, 377–380.

Kinsman, B. (1960) : Surface waves at short fetches and low wind speeds- a field study. vols. 1. 2. 3. *Chesapeake Bay Institute, Tech. Rep.* **XIX**, Ref. 60–1. 581.

Knelman. F., N. Dombrowski, and D. W. Newitt (1954) : Mechanism of the bursting of bubbles. *Nature*, **173**, 261.

Langmuir, I and K. B. Blodgett (1946) : A mathematical investigation of water droplet trajectories. *U. S. Army Forces Technical Report*, No. 5418.

Longuet-Higgins, M. S. (1952) : On the statistical distribution of the heights of sea waves. *Jour. Mar. Res.*, **11**, 245–266.

Mason, B. J. (1955) : Bursting of air bubbles at the surface of sea water. *Nature*, **174**, 470.

May, K. R. (1950) : The measurement of airbone droplets by the magnesium oxide method. *Jour. Sci. Instr.*, **27**, 128–130.

Moore, D. J. (1952) : Measurements of condensation nuclei over the north Atlantic. *Quart. J. Roy. Meteor. Soc.*, **78**, 596–602.

Moore, D. J. and B. J. Mason (1954) : The concentration, size distribution and production rate of large nuclei over the oceans. *Quart. J. Roy. Meteor. Soc.*, **80**, 583–590.

Moore, R. K. and W. J. Pierson, Jr. (1971): Worldwide and wave predictions using a satellite radar-radiometer. *J. Hydronautics*, **5**, 52–60.

Ranz, W. E. and J. B. Wong (1952) : Impaction of dust and smoke particles. *Ind. Engr. Chem.*, **44**, 1371–1381.

Takahashi, T. (1958) : Micro-meteorlogical observations and studies over the sea. Part III Wind profiles and wind waves. *Mem. Fac. Fish. Kagoshima Univ.*, **6**, 37–46.

Tanaka, M. (1970) : Basic study on salt damage (IV) —Distribution of sea-salt particles near the coast—. *Disaster Prevention Res. Inst., Kyoto Univ., Bull,*, No. **13** B, 445–456. (in Japanese).

Tanaka, M. (1971) : Basic study on salt damage (V) —Distribution of sea-salt particles near the coast in the strong wind conditions—. *Disaster Prevention Res. Inst., Kyoto Univ., Bull.*, No. **14** B, 499–519.

Toba, Y. (1959) : Drop production by bursting of air bubbles on the sea surface (II), Theoretical study on. the shape of floating bubbles. *Jour. Oceano. Soc. Japan*, **15**, 121–130.

Toba, Y. (1961) : Drop production by bursting of air bubbles on the sea surface (III), Study by use of a wind flume. *Mem. Coll. Sci. Univ. Kyoto, Ser* A, **29**, 313–344.

Toba, Y. (1965) : On the giant sea-salt particles in the atmosphere. I. General features of the distribution. *Tellus*, **17**, 131–145.

Toba, Y. (1965 a) : On the giant sea-salt particles in the atmosphere. II. Theory of the vertical distribution in the 10-m layer over the ocean. *Tellus*, **17**, 356–382.

Toba, Y. (1966) : On the giant sea-salt particles in the atmosphere. III. An estimate of the production and distribution over the world ocean. *Tellus*, **18**, 132–145.

Toba, Y. (1972) : Local balance in the air-sea boundary processes, I. On the growth process of wind waves. *Jour. Oceanogr. Soc. Japan*, **28**, 109–121.

Toba, Y. (1973) : Local balance in the air-sea boundary Processes. II. Partition of wind stress to waves and

current. *Jour. Oceanogr. Soc. Japan*, **29**, 70–50.

Toba, Y. and M. Chaen (1969) : Observation of sea-water droplets above the sea surface - A study of the air-sea boundary processes with special reference to the breaking of wind waves and sea-water droplets-. *Prel. Rep. Hakuhō Maru Cruise KH*–69–3 (*GARP Cruise*), 28–31. Ocean Res. Inst., Univ. Tokyo.

Toba, Y. and M. Chaen (1973) : Quantitative expression of the breaking of wind waves on the sea surface. *Records Oceano. Works in Japan*, **12**, 1–11.

Toba, Y. and H. Kunishi (1970) : Breaking of wind waves and the sea surface wind stress. *Jour. Oceanogr. Soc. Japan*, **26**, 71–80.

Toba, Y., H. Kunishi, K. Nishi, S. Kawai, Y. Shimada and N. Shibata (1971) : Study of the air-sea boundary processes at the Shirahama Oceanographic Tower Station. *Disaster Prevention Res. Inst., Kyoto Univ., Bull.*, No. **14** B, 519–531 (in Japanese).

Toba, Y., K. Okuda and M. Chaen (1971) : Observation of the breaking of wind waves and the sea-water droplets in relevant to air-sea boundary processes. *Prel. Rep. Haknhō Maru Cruise KH*–70–3 (*2nd GARP Cruise*), 27–29. Ocean Res. Inst., Univ. Tokyo.

Toba, Y. and M. Tanaka (1967) : Simple technique for the measurement of giant sea-salt particles by use of a hand-operated impactor and a chloride reagent film. *Special Contr. Geoph. Inst. Kyoto Univ.*, **7**. 111–118.

Toba, Y. and M. Tanaka (1968): A continuous sampler for sea-salt particles especially of giant class and example of the analysis of data. *Jour. Rech. Atmos.*, **3**, 361–372.

Wiegel, R. L. (1949) : An analysis of data from wave recorders on the Pacific coast of the United States. *Trans. Amer. geophys. Union*, **30**, 700–704.

Woodcock, A. H. (1953) : Salt nuclei in marine air as a function of altitude and wind force. *Jour. Met.*, **10**, 362–371.

Woodcock, A. H. and M. M. Gifford, (1949) : Sampling atmospheric sea-salt nuclei over the ocean. *Jour. Mar. Res.*, **8**, 177–197.

Woodcock, A. H, C. F. Kientzler, A. B. Arons and D. C. Blanchard (1953) : Giant condensation nuclei from bursting bubbles. *Nature*, **172**, 1144–1145.

海面における海塩粒子の生成に関する研究

茶　円　正　明

海面境界過程研究の一環として，海面から生成される海塩粒子に焦点をあわせ，海塩粒子，風，波の組織的観測を行い，海面に接する大気最下層における海塩粒子存在量及び海面よりの生成率を定量的に明らかにした．

海塩粒子の観測は，インパクターと棒捕集器を併用することにより，海塩粒子の塩質量にして 10^{-11}gm から 10^{-7}gm までの広帯域にわたって海塩粒子の存在量を知ることができた．海面に接する大気最下層における海塩粒子個数濃度 θ の鉛直分布は，鳥羽の平衡分布の理論を有効相対湿度を用いて修正することにより表現することができた．海面上 6m 高度における風力ごとに示した平均個数濃度の塩質量分布は塩質量 m（10^{-12}gm 単位）が $\log m = 2.25$ より小さいクラスで直線分布をなしている。その分布は近似的に大気中のエーロソルに関する Junge 分布で表わされる．

個数濃度 θ は，海面の乱れの度合を表わす無次元数 u_*L/ν（u_* は摩擦速度，L は有義波長，ν は動粘性係数）との間に明瞭な関係がみられ，θ は u_*L/ν の増大とともに両対数グラフ上で直線的に増加しており，粒子のかなり局所的な生成状況を反映している大きな塩質量のクラスで，その関係はより明瞭である．

海塩粒子の生成の基準面として，新たに z_1 面を導入した．z_1 面における個数濃度 θ_1 の $\log m$ に対する分布型は，風と波の状態が変化しても変らず同様とみなすことができ，その絶対値が u_*L/ν に比例して変化するとみなすことができる．海塩粒子の生成率 F_1 は，θ_1 から $F_1 = w_s\theta_1$ によって求められた．w_s は海水滴（塩分 35‰）の落下終速度である．F_1 の $\log m$ に対する分布は，$\log m = 3$ に谷を持ち，この塩質量より小さい塩質量と大きい塩質量の双方へ向って増大する．F_1 の $\log m$ に対する分布型も θ_1 のそれと同じく，風と波の状態が変化しても変らず，絶対値が u_*L/ν に比例して変化するとみなすことができる．

塩質量 ($\log m$) の各クラスに対して，個数濃度 θ_1 と生成率 F_1 の値が u_*L/ν の関数として与えられ，また，その近似として，海面状態を風だけの関数とみて，風の関数としての θ_1 と F_1 の値が与えられた．